Microfluidic Screening of Circulating Tumor Biomarkers toward Liquid Biopsy

Article *in* Separation and Purification Reviews · April 2017

DOI: 10.1080/15422119.2017.1320763

2 authors, including:

Nanjing Hao
Duke University
42 PUBLICATIONS **1,472** CITATIONS

SEE PROFILE

Separation & Purification Reviews

ISSN: 1542-2119 (Print) 1542-2127 (Online) Journal homepage: http://www.tandfonline.com/loi/lspr20

Microfluidic Screening of Circulating Tumor Biomarkers toward Liquid Biopsy

Nanjing Hao & John X.J. Zhang

To cite this article: Nanjing Hao & John X.J. Zhang (2018) Microfluidic Screening of Circulating Tumor Biomarkers toward Liquid Biopsy, Separation & Purification Reviews, 47:1, 19-48, DOI: 10.1080/15422119.2017.1320763

To link to this article: https://doi.org/10.1080/15422119.2017.1320763

Accepted author version posted online: 28 Apr 2017.
Published online: 22 May 2017.

Separation & Purification Reviews, 47: 19–48, 2018

ISSN: 1542-2119 print / 1542-2127 online
DOI: https://doi.org/10.1080/15422119.2017.1320763

Microfluidic Screening of Circulating Tumor Biomarkers toward Liquid Biopsy

Nanjing Hao and John X.J. Zhang

Thayer School of Engineering, Dartmouth College, Hanover, New Hampshire, USA

The development of early and personalized diagnostic protocol with rapid response and high accuracy is considered the most promising avenue to advance point-of-care testing for tumor diagnosis and therapy. Given the growing awareness of the limitations of conventional tissue biopsy for gathering tumor information, considerable interest has recently been aroused in liquid biopsy. Among a myriad of analytical approaches proposed for liquid biopsy, microfluidics-based separation and purification techniques possess merits of high throughput, low samples consumption, high flexibility, low cost, high sensitivity, automation capability and enhanced spatio-temporal control. These characteristics endow microfluidics to serve as an emerging and promising tool in tumor diagnosis and prognosis by identifying specific circulating tumor biomarkers. In this review, we will put our focus on three key categories of circulating tumor biomarkers, namely, circulating tumor cells (CTCs), circulating exosomes, and circulating nucleic acids (cNAs), and discuss the significant roles of microfluidics in the separation and analysis of circulating tumor biomarkers. Recent advances in microfluidic separation and analysis of CTCs, exosomes, and cNAs will be highlighted and tabulated. Finally, the current challenges and future niches of using microfluidic techniques in the separation and analysis of circulating tumor biomarkers will be discussed.

Keywords: Microfluidic, separation, purification, tumor biomarker, liquid biopsy

INTRODUCTION

Although great progress has been made in the diagnosis and treatment, cancer is still the leading cause of death worldwide. Cancer metastasis, which occurs in a multistep process including migration and invasion from primary tumor, intravasation and survival in the circulation system, extravasation into distant tissues, and establishing growth in seeded locus, makes it more difficult to successfully treat the disease (1). Therefore, early diagnosis, real-time monitoring and accurate prediction are the most critical issues in cancers. In contrast to conventional tissue biopsy that could take time to process and analyze and be costly, painful, and difficult to obtain, liquid biopsy offers a new and unique opportunity to identify the potential tumor biomarkers for predicting tumor progression and thus have attracted more attentions in recent years (2).

Since then, great efforts have been devoted to the separation and analysis of circulating tumor biomarkers through liquid biopsy (3). Gained from the advances of micro-/nanofabrication approaches, microfluidics-based separation and analysis techniques offer tremendous opportunities in point-of-care disease examination and state-of-art personalized healthcare devices. Typically, microfluidics possesses merits of high throughput, low samples consumption, high flexibility, low cost, high sensitivity, automation capability and enhanced spatio-temporal control (4). These characteristics endow them to serve as a promising tool in tumor diagnosis and prognosis by identifying specific circulating tumor biomarkers.

This review will focus on how the advantages of microfluidics-based separation and purification techniques have been exploited to enhance liquid biopsy analysis. We will emphasize several typical circulating tumor biomarkers

Received 14 October 2016, Accepted 2 April 2017.

Address correspondence to John X.J. Zhang, Thayer School of Engineering, Dartmouth College, 14 Engineering Drive, Hanover, New Hampshire 03755, USA. E-mail: john.zhang@dartmouth.edu

Color versions of one or more of the figures in the article can be found online at www.tandfonline.com/lspr.

from liquid biopsy, including circulating tumor cells (CTCs), circulating exosomes and circulating tumor nucleic acids (ctNAs). The roles of microfluidics in the liquid biopsy will be described. Recent advances of microfluidics in the separation and analysis of circulating tumor biomarkers will be highlighted. Finally, the current challenges and future niches of using microfluidic systems in the separation and analysis of circulating tumor biomarkers will be summarized and discussed accordingly.

CIRCULATING TUMOR BIOMARKERS FOR THE LIQUID BIOPSY

Background of the Liquid Biopsy

Cancer still represents the leading cause of death worldwide, and the major cause of cancer-related death is metastasis. Metastasis is a multistep process in which tumor cells escape from the primary tumor site, enter into the bloodstream and then form to secondary tumor colonies (Figure 1). This metastasis process generally occurs in parallel to the development of the primary tumor, and often before that tumor can be initially detected. Therefore, to be able to effectively improve cancer patient survival, both early real-time diagnosis and the frequent monitoring of patient response to treatment should be carefully and timely performed.

Conventional clinical protocols for cancer diagnosis and treatment are usually based on tissue biopsy, which can be surgical biopsy, radiologically guided biopsy, or endoscopic biopsy. Of these, surgical biopsy is the most commonly used examination technique, which consists of sampling tissues and cells from human body by puncturing organs with a specially designed needle. This technique is invasive, expensive and may introduce clinical risks to the patient. In addition, it also takes time, needs to be consistently evaluated by expert pathologists and thus constitutes a significant barrier for easy and frequent monitoring of cancer progressions. Comparatively, radiologically guided biopsy and endoscopic biopsy techniques have a relatively better operation performance, but both of them make patient suffer from discomfort, and also need expensive equipment and expert pathologists. Therefore, there is an urgent clinical need for the research and development of alternative techniques that can tell cancer information in a simpler and more convenient way compared with tissue biopsy.

The use of biological fluids as a source of noninvasive tumor biomarkers has recently raised a great deal of interest. This so-called liquid biopsy holds great clinical promise, as their noninvasive feature can allow for rapid, facile, economical and repeat sampling. In addition, regarding the increasing awareness of the tumor genetic heterogeneity, liquid biopsy also provides great hope to capture the entire profile of tumor genetic information, which may be probably missed by tissue biopsy. Consequently, liquid biopsy is

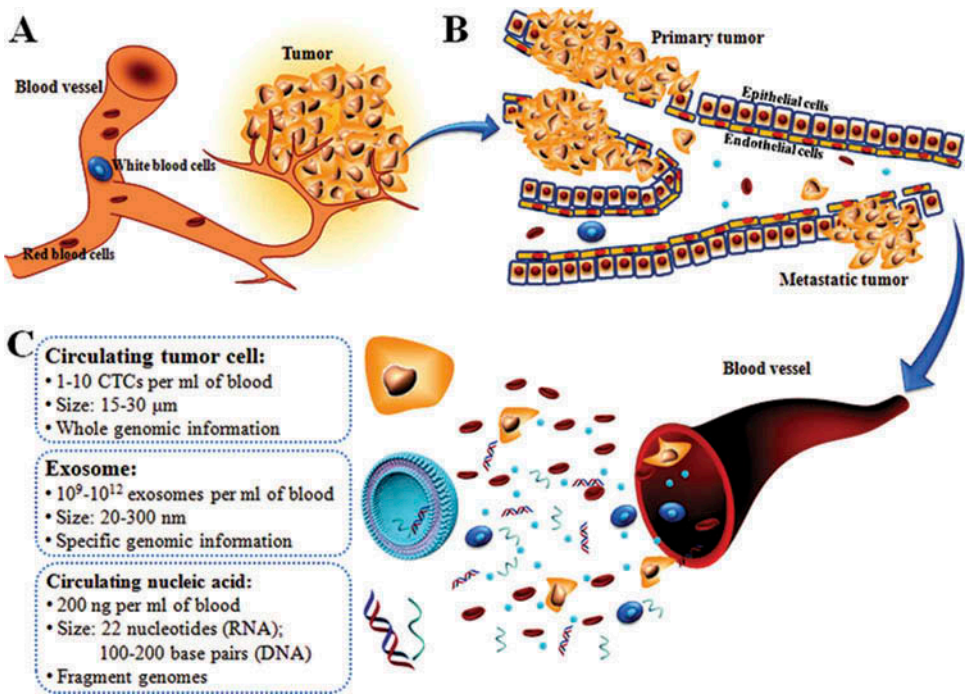

FIGURE 1 Schematic illustration showing cancer progression (A), metastasis (B) and cancer-derived circulating biomarkers presented in the blood of cancer patient (C).

more practical for real-time monitoring and improves the outcome of cancer treatment, allowing for a personalized approach to be taken for each patient. There are various types of biological fluids, such as blood, serum, plasma, saliva, urine, synovial and cerebrospinal fluid, which can be sampled to monitor the level of tumor biomarkers. Peripheral blood and blood-derived products (such as plasma and serum) have been and currently still are the most widely investigated media for liquid biopsy because of their importance in tumor angiogenesis, growth, invasion, and metastasis formation (5). Various analytes with potential implications for cancer diagnosis and treatment can be found in blood (Figure 1). The typical tumor biomarkers include CTCs, circulating vesicle structures (exosomes) and circulating nucleic acids (cNAs).

Categories of Circulating Tumor Biomarkers

CTCs

CTCs are defined as tumor cells circulating in the peripheral blood of patients, shed from either the primary tumor or from its metastasis. The dissemination of tumor cells from primary tumor is the first step of the metastatic process in distant organs, and most patients with epithelial cancers die of metastasis rather than from primary tumors (6). Therefore, identification and characterization of CTCs offer great opportunities to understand the metastatic process and to provide better means of treatment.

Many techniques have been developed in recent years to separate and purify CTCs that are distinct from normal hematological cells based on their biological and physiochemical properties, and trials have proved the prognostic significance of CTCs. In the early stage of these developments, CTCs separation was weighted toward the surface marker expression-based techniques, and epithelial cell adhesion molecule (EpCAM) as a unique CTCs marker was the most frequently employed. Among these, CellSearch™ and GILUPI CellCollector™ are two representative commercial devices that have already been approved by the US Food and Drug Administration and the European Union, respectively, for separation and enumeration of CTCs (7). CellSearch™ relies on the immunomagnetic separation of CTCs using an antibody against EpCAM and performing in a blood draw of 7.5 mL blood, while GILUPI CellCollector™ is a medical wire coated with EpCAM antibodies for *in vivo* CTCs separation and *ex vivo* post-capture analysis *via* insertion in the cubital vein and incubation for 30 minutes.

However, CTCs are exceedingly rare cells, and there are only 1–10 CTCs per milliliter of whole blood containing 10^7–10^9 hematologic cells. This issue together with the heterogeneity of CTCs will obviously hamper the clinically reliable analysis and molecular recognition of CTCs. To meet these challenges, researchers shifted their focus toward microfluidic systems, which will be discussed in detail in the following sections.

Exosome

Circulating tumor exosomes are membrane-bound phospholipid vesicles (20–300 nm in diameter) that are actively secreted by cancer cells (8). Exosomes are first formed as intraluminal vesicles by budding into early endosomes and multivesicular bodies, which will further fuse with lysosomes or the plasma membrane and then release into the extracellular environment to become exosomes (9). Given their specific formation process, exosomes carry a unique cargo of lipids, DNAs, RNAs and proteins that can be distinct, and reflect the cell of origin. Combined with their large abundance (10^9–10^{12} exosomes per milliliter of blood) and ubiquitous presence in body fluids, these tumor-derived exosomes provide significant insights into tumor existence and types, progression and malignancy status, and susceptibility to tumor treatment. Notably, cell-derived exosomes offer attractive possibilities of overcoming biological barriers, which have been considerable challenges for synthetic nanocarriers. Therefore, great research efforts have been dedicated to employ exosome-based drug delivery systems for the treatment of cancer diagnosis and therapy (10).

A variety of strategies and techniques were developed for the separation and purification of exosomes. The most commonly used method is ultracentrifugation. However, this procedure is time consuming and has a relatively low yield (5–25% recovery). Variations on this method, such as adding a sucrose gradient ultracentrifugation step, could achieve higher purity of exacted exosomes but also require a longer processing time. Immunoaffinity-based purification that uses specific antibodies to identify exosome surface markers, such as EpCAM, CD9, CD63, CD81, CD82, Rab5 and annexin, is an alternative strategy for exosomes separation. This technique brings higher purity and recovery rates than centrifugation methods. However, the immunobeads only attach to exosomes that contain the targeted protein, which might not be present in all exosomes in the test sample. Recently, some commercial kits like ExoQuick™, Exo-spin™, Total Exosome Isolation Kit™ and PureExo™ have become available. These kits are easy to use, have high yields, and do not require any expensive ultracentrifugation equipment, but they commonly need a lengthy overnight incubation step and the sample processing procedures are relatively complicated. Given these limitations, conventional separation and purification methods for exosomes are often impractical for clinical examinations that require rapid response, facile operation and high throughput.

Circulating tumor nucleic acids

Nucleic acid molecules are information-rich and are involved in many critical biological processes. Most of nucleic acids in

the body are located within cells, but a small amount of nucleic acids can also be found circulating freely in the blood plasma or serum. The term "Circulating Nucleic Acids" (cNAs) refers to cell-free segments of DNA or RNA found in the bloodstream. The discovery of cNAs in the blood was first reported by Mandel and Metais in 1948, but was initially not widely recognized (11). Evidence that tumor cells can release their nucleic acids into the blood was provided in 1990s (12). cNAs can be used to noninvasively determine the tumor status by decoding the contained genetic and epigenetic information, emerging as a promising liquid biopsy biomarker for cancer early diagnosis and therapy efficacy assessment (13). In particular, cNAs released from tumor cells have recently attracted great attention because they can become detectable in the blood of bladder, breast and colorectal cancer patients before the appearance of other circulating tumor biomarkers, such as CTCs (14).

Circulating DNA was first demonstrated in human blood with concentrations depending on cancer type and progression stage (11). Most cell-free DNA (cfDNA) fragments generating from cell apoptosis are 100–200 base pairs in length, whereas longer fragments (up to 10,000 base pairs) are generated from cell necrosis (15). The concentrations of cfDNA in cancer patient are generally higher than those in healthy individuals (3, 16), indicating that the level of cfDNA can be used directly for cancer screening. Many mutation sites, such as KRAS and EGFR, have been discovered in circulating DNA of cancer patients. Messenger RNA (mRNA) is well-known central to gene expression, which in turn plays a significant role in cellular physiology. Accordingly, cancer disease can often involve changes to the expression of certain genes, which can thus be analyzed through mRNA detection and quantification (17). Since their discovery in the early 1990s (18), micro RNA (miRNA) also holds great promise as distinctive and noninvasive cancer biomarkers (19). miRNAs are small (18–24 nucleotides long), single-stranded, endogenous and nonprotein-coding RNA molecules that regulate gene expression at the posttranscriptional level. Circulating miRNAs play key roles in tumor development and progression, and more than 79 miRNAs have been reported as plasma or serum biomarkers of tumors, such as breast, colon, prostate, melanoma, lung, ovarian, esophageal and gastric cancer (19).

Circulating tumor nucleic acids (ctNAs), especially DNA, mRNA and miRNA, have already been extensively demonstrated their throughout tumor management in the assessment of disease progression, treatment response and prognosis. However, the clinical analysis of ctNAs still faces several key challenges, including relatively low concentration level, great background noise and small size. Conventional methods such as polymerase chain reaction (PCR)-based approaches usually suffer from many drawbacks, including high false-positive rate, low throughput and the lack of reproducibility (17, 20, 21). These challenges set the stage where novel platforms such as microfluidics can play a revolutionary role.

ROLES OF MICROFLUIDICS IN THE LIQUID BIOPSY

Microfluidics is the science and engineering of systems that can precisely manipulate and control small amounts of fluids, usually in the range of microliters (10^{-6} L) to picoliter (10^{-12} L), which are geometrically constrained in the networks of channels with dimensions from a few micrometers up to a millimeter (22). It adopts an integrated, multidisciplinary and intellectual strategy with contributions from physics, engineering, chemistry, materials and biotechnology. Microfluidic systems typically feature high analytical performance, great sensitivity, short analysis time, small volume of analytes, low cost, high system integration, improved potential for automation and control, and disposability (23). This enabling technology holds great promise to open new ways in modern analytical chemistry, pharmaceutics, cell biology, genetics and many other research areas.

Microfluidics normally consists of a set of operation units that allow different analytes to be examined in an easy and flexible manner. These microfluidic components, such as mixer, actuator, reactor, separator, sensor, valve and pump, can be designed and optimized separately for transport processes and fluid control (24). Manufacturing methods of microfluidic devices were developed in the semiconductor and microelectromechanical systems (MEMS) industry; therefore, substrates such as silicon, glass and other various types of polymers are commonly used in their production (25). Silicon is appealing as it is an extensively used material in semiconductor technology with well-known properties (such as chemically and thermally stable) and fabrication methods (such as routine etching and photolithography procedures), which are highly standardized. Glass as an early replacement for silicon is less expensive, negatively charged, chemically stable and transparent, which is especially attractive when optical detection techniques are used. Polymers offer many interesting properties for microfluidic devices, such as inexpensive, disposable, good structural rigidity and strength, facile channels formation *via* soft lithography process, and easy sealing of discrete parts by thermal or adhesive treatment. The choice of polymeric materials is commonly restricted to solvent-resistant materials, such as poly(dimethylsiloxane) (PDMS), poly(methylmethacrylate) (PMMA), thermoset polyesters, polyimide, SU-8 (negative photoresist) and teflon (24, 25).

Inherently, microfluidics could lead them to achieve spatial and temporal control over analytes, which makes it an effective means to interrogate the constituents of biological fluids for disease diagnosis and management. When it comes to exploring the circulating tumor biomarkers in liquid biopsy, all these appealing features would allow microfluidics to revolutionize many aspects of cancer study, such as cancer diagnosis and treatment, personalized medicine and point-of-care devices.

MICROFLUIDICS-BASED SEPARATION AND ANALYSIS OF CIRCULATING TUMOR BIOMARKERS

Separation and Analysis of CTCs

CTCs are shed from primary tumors to flow through the blood stream and may migrate to distant organs to form metastases, which ultimately cause the death of most patients with cancer. Identification and characterization of CTCs provide an effective means to monitor tumor burden and progression (26). Separation and purification of CTCs are generally challenging because they are rare in the blood and possess very heterogeneous features. Microfluidic systems offer many advantages for the separation and analysis of CTCs, especially their high level of system integration, design flexibility, material versatility and advanced degree of automation. For these reasons, a variety of microfluidic devices have been developed to separate and analyze CTCs from a liquid biopsy. These techniques can be simply classified into two main categories: label free–based techniques and immunoaffinity-based techniques (Figure 2). The former is established on the basis of the physical properties of the target cells, such as their size, density, shape, deformability and dielectric properties, whereas the latter utilizes the biochemical properties of the target cells, mainly through protein biomarkers expressed on the cell surface (7, 26).

Label free-based separation and analysis

Many microfluidic techniques for the label-free separation and analysis of cells have been developed (Table 1). According to the physical properties differences, these label-free techniques can be further divided into two subcategories: hydrophoresis (based on the cell size, density, shape, and deformability properties) and dielectrophoresis (based on the cell dielectric property) (27).

Hydrophoresis. Differences in cell size, density, shape and deformability can be exploited for hydrophoresis purpose to separate and purify cells without the need to apply any external force. Hydrophoresis-based methods for label-free capture of cells in microfluidic settings are greatly dependent on the interactions between the species of interest and the microfluidic channel substrates. The cell-microchannel interactions in hydrophoresis systems can be driven by either the continuous channels or the discrete obstacles. The former has a flat microchannel surface, and the flow of cell fractionation in microfluidic channel is mainly controlled by pressure. The latter generally has a periodic array of micrometer-scale posts or ridges, and the critical size cut-off for cell separation can be well controlled. In most cases, hydrophoresis-based label-free cell separation is mediated by the difference in cell size (Figure 3A).

Filtration is a commonly used label-free hydrophoresis technique because it is a relatively straightforward approach for cells separation mainly based on their size property. Microfilters are generally designed with well-defined pore channels to restrict passage of cells above a critical size. Microcavity array represents a typical technique for size-based capture of CTCs (Figure 3B). The size of microcavities is usually less than 10 μm, and because of the larger size of tumor cells than red blood cells (RBCs) (Figure 3A), the blood cells can be filtered out while tumor cells are left behind. The pores of microcavity array can be also designed as many shapes, such as circular (28), oval (29) and rectangular (30). Because each trap is likely to hold only one single cell, the trapped cells can be thus easily detected and counted. Micropost array, different from microcavity array, is an interesting size-based filtration system to

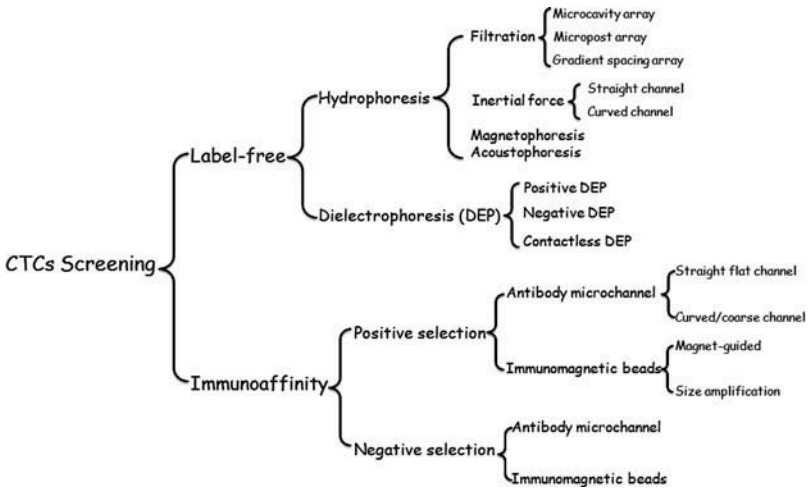

FIGURE 2 Categories of the separation and purification methods for CTCs in microfluidic systems.

TABLE 1
Microfluidics-based separation and analysis of tumor cells

Sample type (tumor cells ratio/concentration)*	*Property used for separation*	*Microfluidic forms*	*Separation methods*	*Flow rate/ volume/time*	*Recovery rate*	*Reference and year*
Label free-based separation and analysis (Hydrophoresis)						
MCF-7, MDA-MB-231, or MDA-MB-435	Magnetism	Glass integrated with magnetophoretic microseparator and μ-EIS	Magnetophoresis (0.2 T)	0.05 mm/s	94.8%	(13) 2006
LNCaP (4–402 cells/mL for circular; 8–86 cells/mL for oval)	Size	PDMS integrated with parylene membrane microcavity array	Filtration (circular/oval pore)	<10 min	~90%	(29) 2007
MCF-7 in MCF-10A (~30%)	Adhesion	PDMS/glass with pillars, perpendicular, and parallel microchannels	Filtration	200 μL/min		(106) 2007
SK-N-MC, SK-N-AS, SK-N-SH, SH-SY5Y, or BE(2)-M17	Size	PDMS/PS/PU with gradient channel gap spacing	Filtration (5, 10, 15, 20 μm spacing array)	1 mL/h		(33) 2009
MCF-7, MDA-MB-231, or HT-29 (100 cells/mL)	Size; deformability; EpCAM; CD45	PDMS/glass with crescent-shaped array	Filtration (20 and 25 μm spacing array)	0.7 mL/h; <2.5 h	>80%	(34) 2009
MCF-7, MDA-MB-231, AGS, N87, HepG2, HuH7, CAL27, or FADU (100 cells/mL)	Size; deformability; EpCAM; CD45; CAM5.2	PDMS/glass with crescent-shaped array	Filtration (20 and 25 μm spacing array)	1–3 mL	>81%	(35) 2010
NCI-H358, MCF-7, SW620, or SNU-1 (10–100 cells/mL)	Size	PDMS integrated with microcavity array	Filtration (circular pore)	0.1–2 mL/ min; 1 mL; 0.5–10 min	98%	(28) 2010
MCF-7	Deformability; EpCAM; CD45	PUMA/glass with a long serpentine channel and 1-D apertures on channel sides	Filtration (aperture); inertial force	12–16 μL/min	~50–90%	(107) 2010
MCF-7 (342 cells/mL)	Size; shape; deformability	Acrylic/PDMS with parylene membrane hexagon-shaped microcavity patch array	Filtration (circular pore)	1 mL; 3–5 min	86.5%	(108) 2011
MCF-7	Size; EpCAM; CD45	PDMS/glass with 2-loop spiral microchannels	Inertial force	1 mL; <15 min	>90%	(109) 2011
MCF-7 (500 cells/mL)	Size; EpCAM; CD45	PDMS/glass with the contraction-expansion microchannels	Inertial force	~400 μL/min	>80%	(39) 2011
MCF-7 or Hela in WBCs (1%)	Size; CD45	PDMS/glass with cell trapping reservoirs	Inertial force	10 μL/min-4.5 mL/min; 1 mL	<43%	(40) 2011
MCF-7 (~500 cells/mL)	Size; EpCAM; Cytokeratin	PDMS/glass with microscale vortices	Inertial force	4.4 mL/min	10–20%	(41) 2011
MCF-7 or Hela ($1:10^4$-$1:10^6$)	Size	PDMS/glass with 6-loop double spiral microchannels	Inertial force	3.33×10^7 cells/min	88.5%	(43) 2012
DU145, PC3, or LNCaP in WBCs	Acoustic; EpCAM; CD45	Glass/silicon with acoustophoresis channel	Acoustophoresis (E_{ac} = 50–200 J/m^3)	100 μL/min	93.6–97.9%	(48) 2012
MCF-10A, PC3, or MDA-MB-231 (~10^6 cells/mL)	Size	PDMS/glass with DLD structure featuring triangular micropost array	Filtration	10 mL/min	>85%	(31) 2012
MCF-7, MDA-MB-231, A549, HepG2, or KYSE150 (~10^3 cells/mL)	Size	PDMS/glass with DLD structure featuring circular or triangular micropost array	Filtration	2 mL/min	99%	(32) 2013
MCF-7 (100 cells/mL)	Size; CD45; EpCAM	PDMS/Glass with ms-MOFF	Inertial force	108–144 μL/ min	>98.9%	(42) 2013
Hela ($1:8 \times 10^7$)	Size	PDMS/glass with 6-loop double spiral microchannels	Inertial force	60 mL/h	90.54%	(44) 2013

Hela; whole blood from liver cancer patient (3–20 cells/3 mL blood)	Size; CD45; EpCAM; Cytokeratin	PDMS/glass with gradient micropillar channel gap spacing	Filtration	0.5–2 mL/h	>90%	(36) 2013
MCF-7 in PBMCs (~10^5/mL); whole blood from metastatic lung cancer (5–88 cells/mL)	Size; EpCAM; CD45; CD133	PDMS/glass with 2-loop spiral microchannels	Inertial force	3 mL/h	>85%	(46) 2013
NCI-H69 or NIC-H82 (1000 cells/mL); whole blood of SCLC patient (0.3–72.7 cells/mL)	Size	PDMS integrated with microcavity array	Filtration (rectangular/ circular pore)	200 μL/min; 1.0–7.5 mL	>80%	(30) 2013
Whole blood from NSCLC or SCLC patient (0–291 cells/7.5 mL)	Size; CD45	CellSearch™ system; PDMS integrated with microcavity array	Filtration (circular pore)	200 μL/min; 3.0–7.5 mL	>68%	(110) 2013
MCF-7, T24, or MDA-MB-231 (500 cells/7.5 mL); whole blood from metastatic breast and lung cancer patient (3–125 CTCs/mL)	Size; CD45; Cytokeratin, CD44; C24	PDMS with 8-loop single spiral microchannel	Inertial force	7.5 mL; <8 min	>80%	(45) 2014
MCF-7 in WBCs (~10%)	Acoustic; EpCAM; CD45	PDMS integrated with tilted interdigitated transducers	Acoustophoresis (~30 dBm)	1.1 mL	71%	(49) 2014
MCF-7, HeLa, LNCaP, or UACC903M-GFP in WBCs (1:6×10^3-1:10^5)	Acoustic; CD45; Cytokeratin	PDMS integrated with tilted interdigitated transducers	Acoustophoresis (~37.5 dBm)	1.2 mL/h	>83%	(50) 2015
Label free-based separation and analysis (Dielectrophoresis)						
HL-60 (2:3)	Dielectric	Gold polynomial electrode array on glass slide with rotating electrical field generator	DEP (5 V_{pp}, 20–200 kHz)	30 μL	80%	(111) 1994
MDA-231 (1:3)	Dielectric; size	Gold polynomial electrode array on glass slide with rotating electrical field generator	DEP (5 V_{pp}, 20–200 kHz)	30 μL	>95%	(112) 1995
HL-60 in PBMCs	Dielectric	DEP-FFF with microelectrode array	DEP (0.88 V_{rms}, 25 kHz)	250 μL		(64) 1997
MDA-231 (1:3-1:3×10^5)	Dielectric; size; shape	Gold polynomial electrode array on glass slide with rotating electrical field generator	DEP (2 V_{rms}, 50 kHz)	5 μL/min	>95%	(113) 1997
HeLa in PBMCs	Dielectric	Silicon/glass with circular platinum electrodes	DEP (6 V_{pp}, 30 kHz)	200 μL/min; ~3 min		(58) 1998
MDA-435 in $CD34^+$ stem cells (2:3)	Dielectric	DEP-FFF with interdigitated electrode array	DEP (4 V_{pp}, 10 kHz)	50 μL; <12 min	>99% (for $CD34^+$ fractions)	(53) 1999
MDA-435 (2:3)	Dielectric; density	DEP/G-FFF with interdigitated electrode array	DEP (1.4 V_{rms}, 5 kHz)	10 μL; 5 min	>98%	(54) 1999
MDA-435 in $CD34^+$ stem cells (1:1); MDA-435 in T-lymphocytes (2:3)	Dielectric	DEP-FFF with interdigitated electrode array	DEP (4 V_{pp}, 15–40 kHz)	50 μL; <15 min	~70%	(55) 2000
HTB in SH-SY5Y (10–20%)	Dielectric	PMMA with circular platinum electrode array	DEP (8 V_{pp}, 400 kHz)	~500–15,000 cells	>47%	(59) 2002
K562 in RBCs	Dielectric	Cylinder-shaped DEP cage with a printed circuit board device	DEP (6 V_{pp}, 100 kHz)		100%	(60) 2003
MDA-231, MDA-435, MDA-468, HL-60, SW-756, Jurkat, and SKI	Dielectric	Gold electrode array on electrosmear glass slide with multifrequency signal generator	DEP (0–5 V_{pp}, 0–1200 kHz)	20 μL		(114) 2005
P19 in RBCs (1:1)	Dielectric	Pyrex with fan-shaped 3D-asymmetric microelectrodes	DEP (8 V_{pp}, 5 MHz)	300 μm/s	81.5%	(61) 2005
A549	Dielectric	PDMS/glass with a serpentine-shape pneumatic micropump device	DEP (15 V_{pp}, 16 MHz)	3 μL/min; 100 μL	~80%	(115) 2007

(*Continued*)

TABLE 1
(Continued)

Sample type (tumor cells ratio/concentration)*	*Property used for separation*	*Microfluidic forms*	*Separation methods*	*Flow rate/ volume/time*	*Recovery rate*	*Reference and year*
MDA-MB-231	Dielectric; size; cell-cycle phase	Polyimide with DACSync device	DEP (20 V_{pp}, 800 kHz)	200–400 μL/h	96% (G_1 phase)	(116) 2007
MDA-MB-435 from tumor xenografts in PBMCs (20%)	Dielectric	Electrosmears-based gold microelectrode array	DEP (3.3 V_{pp}, 10–920 kHz)	100 μL/min	~75%	(117) 2008
MCF-7 (100%, size-based DEP separation)	Dielectric; size	PDMS with rectangular and triangular hurdle channels	DEP (0–180 V)		~100%	(118) 2008
MCF-7 in MCF-10A	Dielectric	Glass with DACS having fan-shaped electrode	DEP (8 V_{pp}, 48 MHz)	290 μm/s	86.67%	(62) 2009
MDA-MB-435, MDA-MB-468, MDA-MB-231 in PBMCs ($1:10^3$–$1:10^5$)	Dielectric; size	DEP-FFF chamber with an interdigitated gold-on-copper electrode	DEP (2.8 V_{pp}, 60 kHz); Inertial force	1.5–12 mL/ min; <15 min	>90%	(56) 2009
THP-1, MCF-7, and MCF-10A	Dielectric	PDMS/glass with a contactless DEP device	DEP (250 V_{rms}, 85 kHz)	10–15 μL/min		(66) 2009
HCT116 in HEK 293 and *E.coli*	Dielectric	Plastic with a wedge microfluidic chip	DEP (16 V_{pp}, 100 kHz)	0.1 μL/min	~90%	(63) 2010
B16F10 clones	Dielectric	Castellated gold electrode array	DEP (5 V_{pp}, 200–400 kHz)	500 cells per frequency	<70%	(57) 2010
Jurkat and HeLa	Dielectric	Silicon with a guided DEP microchannel	DEP (4 V_{rms}, 1 MHz)	0.45 μL/min; 50 μL		(119) 2010
MCF-7 in RBCs and WBCs (0.1%)	Dielectric; EpCAM; CD45	PDMS/glass with p-MOFF and DEP microchannels	DEP (10 V_{pp}, 900 kHz)	126 μL/min	75.81%	(65) 2011
MDA-MB-231 in MCF-7 and MCF-10A	Dielectric	PDMS/glass with a contactless DEP device	DEP (30 V_{rms}, 164 kHz)	0.02 mL/h	>90%	(67) 2011
MDA231 ($1:10^4$–$1:10^6$)	Dielectric	PDMS/quarts with interdigitated comb-like electrodes	DEP (20 V_{pp}, 10–50 kHz)	0.1 mL/h; <1 h	95–98%	(120) 2011
SKOV3 or MDA-MB-231 in PBMCs (~$1:10^3$–$1:10^4$)	Dielectric	ApoStream™ having a polyimide film sheet with copper and gold electrodes	DEP (2–4.5 V_{pp}, 900 kHz)	18–25 μL/ min; 60 min	~75%	(68) 2012
PC-3 or OEC-M1 in leukocyte (10%)	Dielectric; EpCAM; CD45	PDMS/glass with an optically-induced DEP device	DEP (2–7 V_{pp}, 50–1500 kHz)	0.1 μL/min; 1 μL	~60–80%	(121) 2013
Immunoaffinity-based separation and analysis (Positive selection)						
NCI-H1650 (50-50,000 cells/mL); whole blood from metastatic lung, prostate, pancreatic, breast, and colon cancer patient (5–1281 cells/mL)	EpCAM; CD45; Cytokeratin	Silicon wafer with circular micropost array	Antibody micropost	1–2 mL/h	*NCI-H1650*: >60%; *Patient*: 99%	(74) 2007
MCF-7 (10–250 cells/mL)	EpCAM	PMMA with the sinusoidally shaped capture channels and an integrated conductivity sensor	Antibody microchannel; Inertial force	>1 mL; <37 min	>97%	(72) 2008
MCF-7 (5–1250 cells/mL)	EpCAM	Silicon wafer with nanopillar array	Antibody nanopillar	1 mL	>40%	(76) 2009
CCL-119 in PBS (5×10^5–1×10^6 cells/mL)	Aptamer sgc8	PDMS/glass with aptamers-immobilized microfluidic channel	Aptamer microchannel	200 nL/s; 48 μL	>80%	(80) 2009
CCL-119, CRL-1596, and CRL-2631 in PBS (1×10^6 cells/ mL)	Aptamer sgc8; TD05; Sgd5	PDMS/glass with aptamers-immobilized serpentine microfluidic channel	Aptamer microchannel	300 nL/s	96%	(81) 2009
MCF-7 in Jurkat (4:6)	5D10 mAb; Fibronectin	PDMS/glass with patterned immunomagnetic beads array	Antibody microchannel	10 nL/s	85%	(78) 2010
PC3 (500–1000 cells/mL); Whole blood from prostate cancer patient (12–3167 cells/mL)	EpCAM; CD45; PSA	PDMS/glass with microvortex-generating herringbone chip	Antibody microchannel	1.5–2.5 mL/h	~93%	(73) 2010

SW620 or HT29	EpCAM	PMMA with the sinusoidally shaped capture channels and an integrated conductivity sensor	Antibody microchannel; Inertial force	2 mm/s; 1 mL; <40 min	96%	(71) 2011
PC-9 or MCF-7	EpCAM; CD45	MACS^{TM} MS-column coupled with flow cytometer	Immunomagnetic beads for labeling	1 mL	95.8%	(122) 2011
MCF-7 (50–1000 cells/mL)	EpCAM; CD45; Cytokeratin	PDMS/Silicon with a serpentine chaotic mixing channel	Antibody nanopillar	0.5–7 mL/h	>95%	(70) 2011
COLO205 or SKBR3 (200 cells/2.5 mL)	EpCAM; CD45; Cytokeratin	PDMS/glass with parallel-arrangement magnet array	Immunomagnetic beads for labeling	10 mL/h	>86%	(84) 2011
KG1a (1:1); whole blood from breast, prostate, lung, and ovarian cancer patient (20–704 cells/3.75 mL)	EpCAM; Selectin; PSA	Micro-Renathane microtube	Antibody microchannel	4.8 mL/h	~50%	(69) 2012
PC3 in WBCs (1:250)	EpCAM	PDMS with a fluid-permeable porous polycarbonate membrane	Antibody microchannel	6 mL/h	~70%	(123) 2012
M6C (2–80 cells/mL)	EpCAM; CD45; Cytokeratin	PDMS/glass with micropillar array channel	Immunomagnetic beads for labeling	20 μL/min; 5 min	90%	(77) 2012
MCF-7 or MDA-MB-231 (100 cells/mL)	EpCAM; Size	Silicon/glass with MOA filter	Immunobeads for size amplification	20 μL/min; 1 mL	92%	(51) 2012
MCF-7 or CKBr-3; whole blood from metastatic breast cancer (11–105 cells/7.5 mL)	EpCAM; Her2; Cytokeratin, CD44; CD24	PDMS/glass with eDAR-based microfluidic chip	Fluorescent-activated cell sorter	10–80 μL/min	>93%	(124) 2012
MCF-7 (0–1000 cells/mL)	EpCAM	PDMS/glass with packed bed microfluidic channel containing a weir	Immunobeads for retention	0.2 mL/h	30–70%	(125) 2012
MCF-7 or DMS-79 (100 cells/mL)	EpCAM; size; CD45; Cytokeratin	Silicon/glass with parallel microfluidic channel	Immunobeads for size amplification; Filtration	1 mL	>89%	(95) 2012
MCF-7 in Jurkat (1:10^{7})	EpCAM	PMMA with disk-based microchannels and multistage concentric-circular magnet	Immunomagnetic beads for labeling; Inertial force	~30 min	80%	(92) 2012
MCF-7 (1-10 cells/mL)	EpCAM	PDMS/glass with DLD structure featuring triangular micropost array and fishbone structure chamber	Antibody microchannel	9.6 mL/min	90%	(75) 2013
PC3-9, SKBR3, MDA-MB-231, MCF10A-LBX1; whole blood from prostate, lung, pancreas, breast, and melanoma cancer patient (>0.5 cell/mL)	EpCAM; Her2; Estrogen receptor; Cytokeratin; size	PDMS/glass integrated with CTC-iChips	Immunomagnetic beads for labeling; DLD; Inertial force	6–12 mL	>77.8%	(93) 2013
MCF-7	EpCAM; CD45; Cytokeratin	Silicon/glass with TRAB microfilter	Immunobeads for size amplification	100 μL/min	93%	(97) 2013
MCF-7 or MDA-MB-231 (125–2000 cells/mL)	EpCAM	PDMS/glass with a vortex micromixer and consecutive wavy ducts	Immunobeads for size amplification	100–600 μL/min	*MCF-7*: 95.8%; *MDA-MB-231*: 15%	(96) 2013
SkBr3, PC3, or Colo205 (200 cells/2.5 mL); whole blood from breast, prostate, and lung cancer patient (>1 cells/5 mL)	EpCAM; CD45; Cytokeratin	PDMS/glass with inverted channel and parallel-arrangement magnet array	Immunomagnetic beads for labeling	2.5 mL/h	>94%	(85) 2013
SK-BR-3 (10–10^{4} cells/0.2 mL); Whole blood from breast and lung cancer patient (2–41 cells/0.2 mL)	EpCAM; CD45; Cytokeratin	Glass with a ferromagnetic wire array	Immunomagnetic beads for labeling	5 mL/h	90%	(94) 2013
COLO 205, SK-BR-3, or A-431 (~100–200 cells/2.5 mL)	EpCAM; Cytokeratin; HER2; EGFR	PDMS/glass with inverted channel and parallel-arrangement magnet array	Immunomagnetic beads for labeling	2.5 mL/h	~45–93%	(91) 2013

(*Continued*)

TABLE 1
(Continued)

*Sample type** *(tumor cells ratio/concentration)*	*Property used for separation*	*Microfluidic forms*	*Separation methods*	*Flow rate/ volume/time*	*Recovery rate*	*Reference and year*
COLO 205 (~150 cells/2.5 mL)	EpCAM; CD45; Cytokeratin	PDMS/glass with inverted channel and micromagnet array	Immunomagnetic beads for labeling	2.5 mL/h	98%	(90) 2015
MCF-7, PC3, SK-BR-3, or COLO 205 (200 cells/10 μL)	EpCAM; CD45; Cytokeratin	PDMS/glass with micromagnet array	Immunomagnetic beads for labeling	2.5 mL/h	97%	(87) 2015
COLO 205 (~150 cells/2.5 mL)	EpCAM; CD45; Cytokeratin	PDMS/glass with inverted channel, micromagnet array, and spacered magnets	Immunomagnetic beads for labeling	2.5 mL/h	95.6%	(88) 2016
Immunoaffinity-based separation and analysis (Negative selection)						
MCF-7 in PBMCs (~47:10^6)	CD45; Cytokeratin	PMMA with disk-based microchannels and multistage concentric-circular magnet	Immunomagnetic beads for labeling; Inertial force	~30 min	60%	(101) 2011
MCF-7 or MDA-MB-231 in Jurkat; Whole blood from metastatic breast, lung, and gastric cancer patients (1–51 cells/mL)	CD45; Cytokeratin	PDMS/glass with GASI chip having asymmetric herringbone microchannels	Antibody microchannel	10–40 μL/min	3.92–100%	(99) 2013
PC3-9, SKBR3, MDA-MB-231, MCF10A-LBX1; whole blood from prostate, lung, pancreas, breast, and melanoma cancer patient (>0.5 cell/mL)	CD45; Cytokeratin; CD15; size	PDMS/glass integrated with CTC-iChips	Immunomagnetic beads for labeling; DLD; Inertial force	6–12 mL	>77.8%	(93) 2013
WM164, MB231, PC9, PC3-9, SKBR3, or MCF10A-LBX1 (1000 cells/mL); whole blood from breast and pancreatic cancer patient	CD45; CD66b; Size	PDMS/glass integrated with CTC-iChips	Immunomagnetic beads for labeling; DLD; Inertial force	8 mL/h	97%	(105) 2014
MCF-7 or NCI-H1975 (5–50 cells/mL)	CD45; Cytokeratin	PMMA integrated with microslit membrane mesh	Immunomagnetic beads for labeling; filtration	~60 min	>90%	(103) 2014
MCF-7 in WBCs	CD45	PDMS/glass with serpentine microfluidic channels	Roughened antibody microchannel	2 μL/min; 200 μL	~50%	(100) 2015
HCT116 in PBMCs (3–250 cells/2 mL blood); whole blood from colorectal cancer patient	CD45; Cytokeratin; EpCAM; CD44; CD47	Magnetic cell separator coupled with flow cytometer	Immunomagnetic beads for labeling		>61%	(102) 2015
NCI-H1975, SW48, PC3, MCF-7, or Jurkat (1–25 cells/mL)	CD45; Cytokeratin	PMMA integrated with permanent magnet array and microslit membrane mesh	Immunomagnetic beads for labeling; filtration	500 μL/min; 2 mL	>80%	(104) 2016

*Cell line was used to spike into whole blood that was collected from healthy body, unless specially indicated.

DACS: Dielectrophoresis-activated cell sorter; DACSync: Dielectrophoresis-activated cell synchronizer; DEP/G-FFF: Dielectrophoretic/gravitational field-flow fractionation; DEP: Dielectrophoresis; DEP-FFF: Dielectrophoretic field-flow fractionation; DLD: Deterministic lateral displacement; E_{ac}: Acoustic energy density; eDAR: Ensemble-decision aliquot ranking; EpCAM: Epithelial cell adhesion molecule; GASI: Geometrically activated surface interaction; mAb: Monoclonal antibodies; MOA: Multi-obstacle architecture; ms-MOFF: Multi-stage multi-orifice flow fractionation; NSCLC: Nonsmall cell lung cancer; p-MOFF: Parallel multi-orifice flow fractionation; PBMCs: Peripheral blood mononuclear cells; PBS: Phosphate buffered saline; PDMS: Polydimethylsiloxane; PMMA: Poly(methyl methacrylate); PS: Polystyrene; PSA: Prostate-specific antigen; PU: Polyurethane; PUMA: Polyurethane-methacrylate; RBCs: Red blood cells; SCLC: Small cell lung cancer; taSSAW: Tilted-angle standing surface acoustic waves; TRAB: Tracheal carina-inspired bifurcated; V_{pp}: Peak-to-peak voltage; V_{rms}: Root mean square voltage; WBCs: White blood cells.

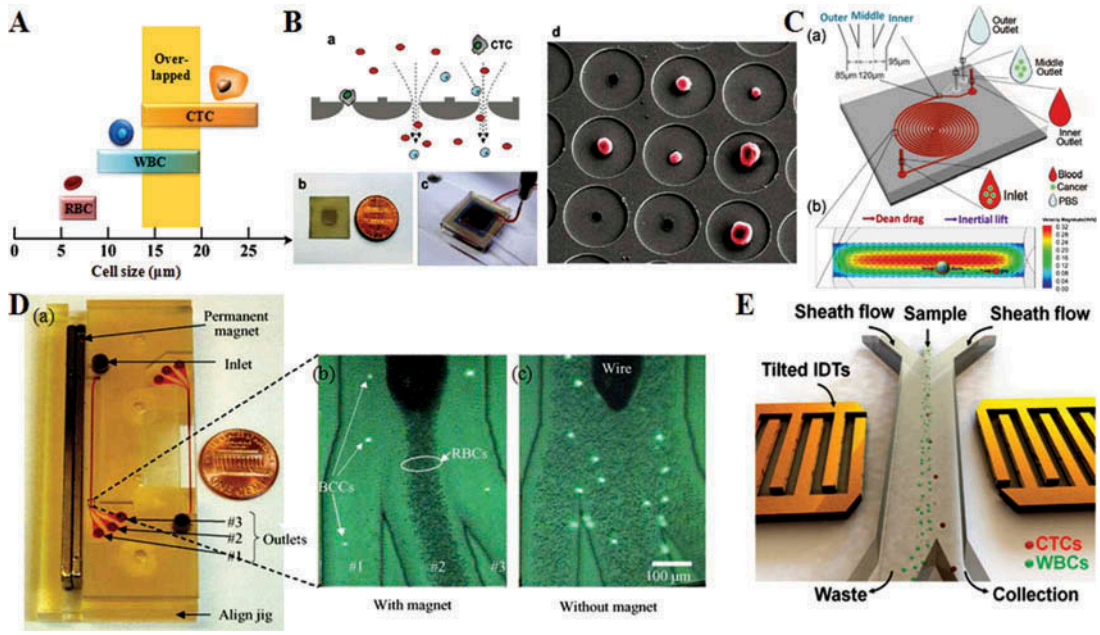

FIGURE 3 Hydrophoresis-based microfluidic systems for cell analysis. (A) Size comparison of CTCs with hematologic white blood cells (WBCs) and red blood cells (RBCs). Adapted from Ref. (51); (B) Size-selective microfiltration array-based CTC recovery device. (a) Schematic image of CTC recovery device using the size-selective microfiltration array. (b) and (c) Photographs of the microfiltration array and CTC recovery device equipped with the array, respectively. (d) SEM image of MCF-7 cells trapped on the microfiltration array. The microcavities are 9 μm in size with a 60-μm pitch. Adapted from Ref. (28); (C) Inertial force–based size separation of CTCs in spiral microfluidic channels. (a) Schematics of the microfluidic cell sorter containing 6-loop double spiral microchannels with one inlet and three outlets for cell separation. (b) Illustration of the two counter-rotating Dean vortices forming in the top and bottom halves of the channel. The black arrows represent the velocity field in the cross section. Adapted from Ref. (43); (D) Magnetophoresis-based breast cancer cells (BCCs) separation from RBCs. (a) Top view of the fabricated paramagnetic capture mode (PMC) microseparator. Fluorescently probed BCCs passing through the microchannel of the PMC microseparator at (b) an average flow velocity of 0.05 mm/s with an external magnetic flux of 0.2T, and (c) an average flow velocity of 0.05 mm/s without the external magnetic flux. Adapted from Ref. (13); (E) Illustration of taSSAW-based acoustophoretic cell separation. Adapted from Ref. (50).

separate cells using a principal known as deterministic lateral displacement (DLD), as the displacement of cells perpendicular to primary flow is determined by the pattern of the array (31, 32). Cells below a critical size follow streamlines through the array gaps with no net displacement from the original streamline, whereas cells above the critical size are "bumped" laterally to cross sequential streamlines in each row at an angle predetermined by the post offset distance. The critical cell size for fractionation depends on the gap between posts and offset of posts, which also means that DLD micropost shape is an important parameter for determining the separation and purification efficiency (32). Compared to the microcavity array and micropost array, the gradient gap spacing microchannel array-based filtration is a much more appealing technique, which can be used for the separation of various blood cell types due to their inherent size differences (33–36). This kind of microfluidic system with successively narrower gap widths between the columns can retain increasingly smaller cells; therefore, tumor cells, white blood cells (WBCs), RBCs and cell fractions can be specially separated.

Inertial forces generated by the flow in microfluidic channels can be applied as a rapid and label-free strategy to separate and purify CTCs. There are two kinds of microchannel forms for inertial force-based separation: straight channels and curved channels (37, 38). In a straight channel, fluid shear generates lateral forces, which cause transverse inertial migration of cells. In a curved channel, centrifuge forces overlap with the inertial forces and generate a double recirculation in the transversal section of the microchannels (Dean drag) (27). Inertial migration in a straight channel for cell separation generally consists of different kinds of trapping reservoirs (39–42). When cells are flowing through the microfluidic channel, they need to reach equilibrium at a well-defined distance between the center of the cell and the microchannel wall due to the inertial lateral forces. Once the cells reach the reservoir's area, larger-sized cells are pushed toward a vortex generated in the reservoir and thus trapped within, while smaller-sized cells can be flushed toward the outlet. Inertial force–based cell separation in a curved channel is often provided by using spiral microfluidic system (Figure 3C) (43–46). In this case, when cells are flowing through the microchannel, the dominant inertial force and a secondary rotational flow field perpendicular to the original flow direction (Dean flow) will lead the smaller-sized particles to migrate in the direction of the outer half of the

channel, while the larger-sized particles can migrate toward the inner channel wall. Therefore, this so-called Dean flow field fractionation technique can be applied to separate cells with short acting time and high selectivity.

Magnetophoresis and acoustophoresis, in addition to filtration and inertial force, are another two appealing label-free techniques for cells separation based on their intrinsic magnetic moment and acoustic properties, respectively. Magnetophoresis-based separation involves the manipulation of cells in a fluid medium under the influence of an external magnetic field. Magnetophoresis provides an alternative means for gentle cells separation in their natural milieu that could be highly specific and highly sensitive without the need of any complicated or expensive equipment (47). This kind of microfluidic separation systems employs the intrinsic paramagnetic properties of deoxyhemoglobin that was found only in erythrocytes. In contrast, other cell types, such as WBCs and tumor cells, are generally considered with diamagnetic properties. Therefore, RBCs and other biological components will be moving in opposite directions due to the force created by the external magnetic field (Figure 3D) (13). Similarly, acoustophoresis in a flow channel is achieved by establishing a standing acoustic field, which will push cells toward regions with minimal acoustic radiation pressure (pressure nodes). Cells with different size, shape and other physical properties will experience different acoustic radiation forces and require different times to migrate to the pressure nodes, thus providing clear identifiers for separation. The standing surface acoustic waves for acoustophoresis in microfluidic systems can be controlled at a position parallel to the fluid flow direction (48), or with certain angle (49, 50). The latter system (so-called tilted-angle standing surface acoustic waves, taSSAW) could make the cells in a fluid medium experience both the acoustic radiation force and the laminar drag force, and thus lead to better separation sensitivity (Figure 3E) (49,50).

Dielectrophoresis. Dielectrophoresis (DEP)-based cells separation is a technique by which cells are induced to move by the application of a nonuniform electric field due to the interactions of the cells' dipole and spatial gradient of the electric field (Table 1) (52). When electric fields are applied to cells, they become polarized. This induced polarization can then interact with the applied field, resulting in each kind of cells experiencing a unique net electrical force. The magnitude of this net force depends on many factors, such as cell membrane property, cell size, cytoplasmic property, the frequency and strength of the electric field, and the fluid medium property. If cells are more polarizable than the suspending medium, they will be attracted toward the regions of higher electric fields and retained at the electrode surface; this motion is called positive DEP (pDEP) (Figure 4A). Conversely, if cells are less polarizable than the suspending medium, they will move to the regions of lower electric fields and then be eluted by the flow; this motion is called negative DEP (nDEP) (Figure 4A). In the case of CTCs separation from blood, electrophoretic

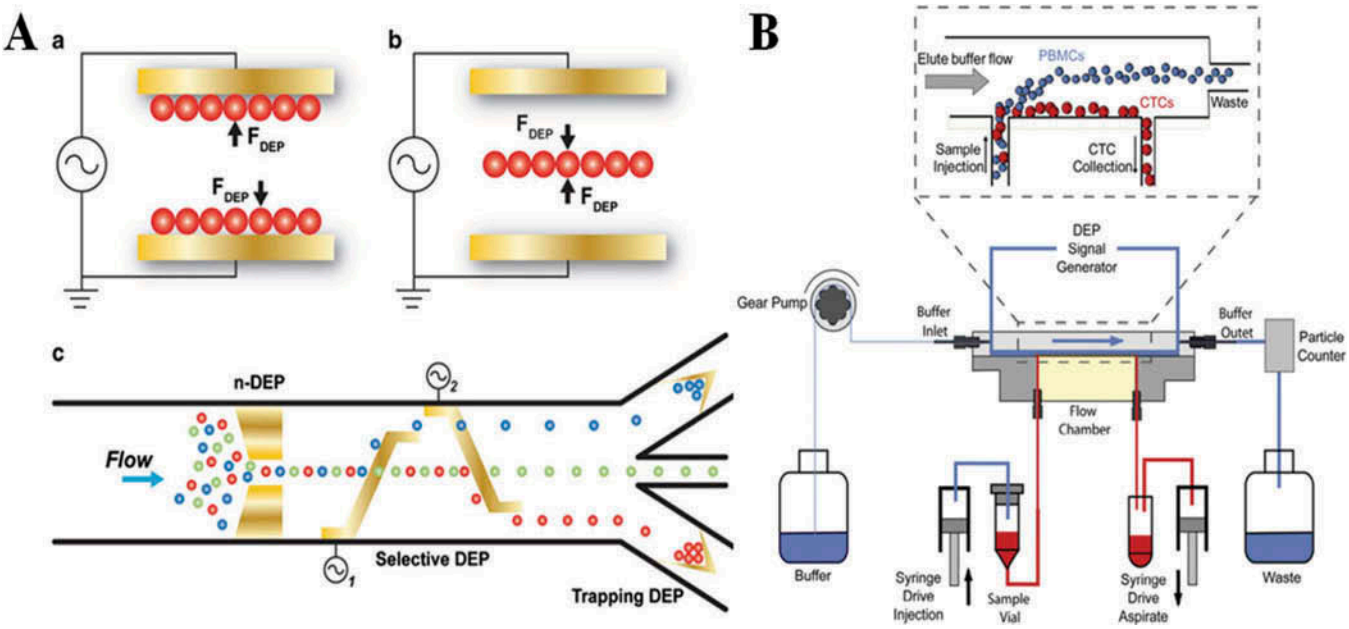

FIGURE 4 Dielectrophoresis-based microfluidic systems for cell analysis. (A) Dielectrophoresis (DEP) separation can be positive (pDEP) (a) or negative (nDEP) (b), which affects the positioning of cells within a field. (c) Examples of DEP utilized in microfluidic systems in a variety of arrangements. Adapted from Ref. (38); (B) A continuous flow DEP microfluidic cell-sorting device. Adapted from Reference (68).

mobility generally distinguishes tumor cells with attraction toward the electrode, and normal blood cells migrate in the electric field into the eluent.

Metallic microelectrodes with various shapes, such as interdigitation (53–56), castellate (57), circular (58, 59), cylinder (60), fan (61, 62) and wedge (63), can be easily patterned on a microfluidic wafer using conventional lithography techniques for DEP-based cells separation. Therefore, a number of DEP-based microfluidic devices have been employed to separate tumor cells (Table 1). Among these, field flow fractionation (FFF) and multi-orifice flow fractionation (MOFF)-integrated DEP techniques bring many new features for CTCs separation. FFF is an analytical technique to achieve cell fractionation that uses the velocity gradient of a hydrodynamic flow profile. Cells in a long and narrow microfluidic channel are forced toward the bottom wall of the chamber when a force field normal to the flow direction is applied. In this so-called DEP-FFF system, which is the combination of dielectrophoretic levitation of cells with FFF technique, cells can reach equilibrium positions at different heights depending on their electric properties, achieving high cell separation efficiency and throughput (53–56, 64). The termed MOFF technique involves the lateral movement of cells according to their size due to hydrodynamic inertial force. This integrated DEP-MOFF system that combines both hydrodynamic and dielectrophoretic separation techniques can result in fast (with respect to flow rate) and efficient performance (65).

Compared to conventional metallic microelectrodes, the contactless DEP (cDEP) that utilizes fluidic electrode channels with filled high-conductivity solution is also a promising technique for label-free cells separation. This technique eliminates cell-electrode contact, minimizes the contamination of the biological samples, and reduces the fabrication steps and costs. cDEP has successfully been proven to selectively separate cells (66, 67). In addition, it is noted that a commercial DEP-based microfluidic system for CTCs separation, ApoStream™, has already been launched (68). In this system, the sample is introduced through a port located in the floor of the flow chamber at the same upstream end as the elution buffer, and cancer cells can be collected through another port located downstream from the sample inlet port (Figure 4B). When cells encounter the DEP field, the DEP force will pull cancer cells toward the chamber floor and repel other cells as they traverse the electrode. Therefore, cancer cells traveling close to the chamber floor will be withdrawn through the collection port, while other blood cells traveling at greater heights will be carried beyond this port and exit the chamber to the waste container *via* a second outlet port (Figure 4B) (68).

Immunoaffinity-based separation and analysis

CTCs can also be distinguished from background cells based on their surface markers. Many techniques have thus been developed for the separation and analysis CTCs (Table 1). These immunoaffinity-based techniques can be further classified into two categories: positive selection (based on the capture of target tumor cells and the elution of nontarget cells) and negative selection (based on the capture of nontarget cells and the elution of target tumor cells).

Positive Selection. Positive selection, which is established by using the specific epitopes expressed on the tumor cell surface, has been extensively developed (Table 1). EpCAM is the most commonly used epitope for all immunoaffinity-based positive selection methods. According to the binding site differences, positive selection can be realized by either modifying microchannel substrate surface with antibodies or manipulating antibodies-conjugated micrometer-sized magnetic beads.

EpCAM antibody-coated microfluidic channel systems have attracted a great interest in recent years. When CTCs flow across the microchannels, the interactions between these binding ligands and CTCs surface epitopes can capture and retain the tumor cells, and the remaining blood components can be carried away by the flow. The captured tumor cells on the microfluidic channel surface can then be dislodged and collected for further analysis. The biggest challenge in conventional straight flat microfluidic channel is its limited surface area for anchoring ligands (69). Given the larger surface area in microfluidic channel will certainly provide more possible interaction sites to increase the chances of CTCs capture, different kinds of curved and/or coarse channels have been specially designed, such as serpentine-shaped channel (70–72), herringbone array (73), micropost array (74, 75), nanopillar array (70, 76, 77) and immunobeads array (78, 79). All these strategies, compared to conventional straight flat microfluidic systems, could generate higher surface area inside the microchannels for binding more target ligands and thus show better capture efficiency of tumor cells (Figure 5A). It is noted that besides EpCAM antibody, aptamers that are single-strand nucleic acid oligomers for binding target proteins, peptides and amino acids can also endow aptamers-coated microchannels with high specificity and affinity for tumor cell separation and enrichment (80, 81).

Immunomagnetic-based cell separation, in which micrometer-sized magnetic beads are selectively attached to the tumor cells, is also a common technique for CTCs enrichment due to its high sensitivity and ability to handle a large range of volumes without the need of surface modification inside of microfluidic channels (82, 83). Various immunomagnetic microfluidic devices were developed in our laboratory, and the magnetic field design from the integrated magnets in microfluidic systems was also optimized for controlling capture of tumor cells (Figure 5B) (84–91). There are generally two kinds of roles for magnetic beads in immunomagnetic-based cell separation. One is to label

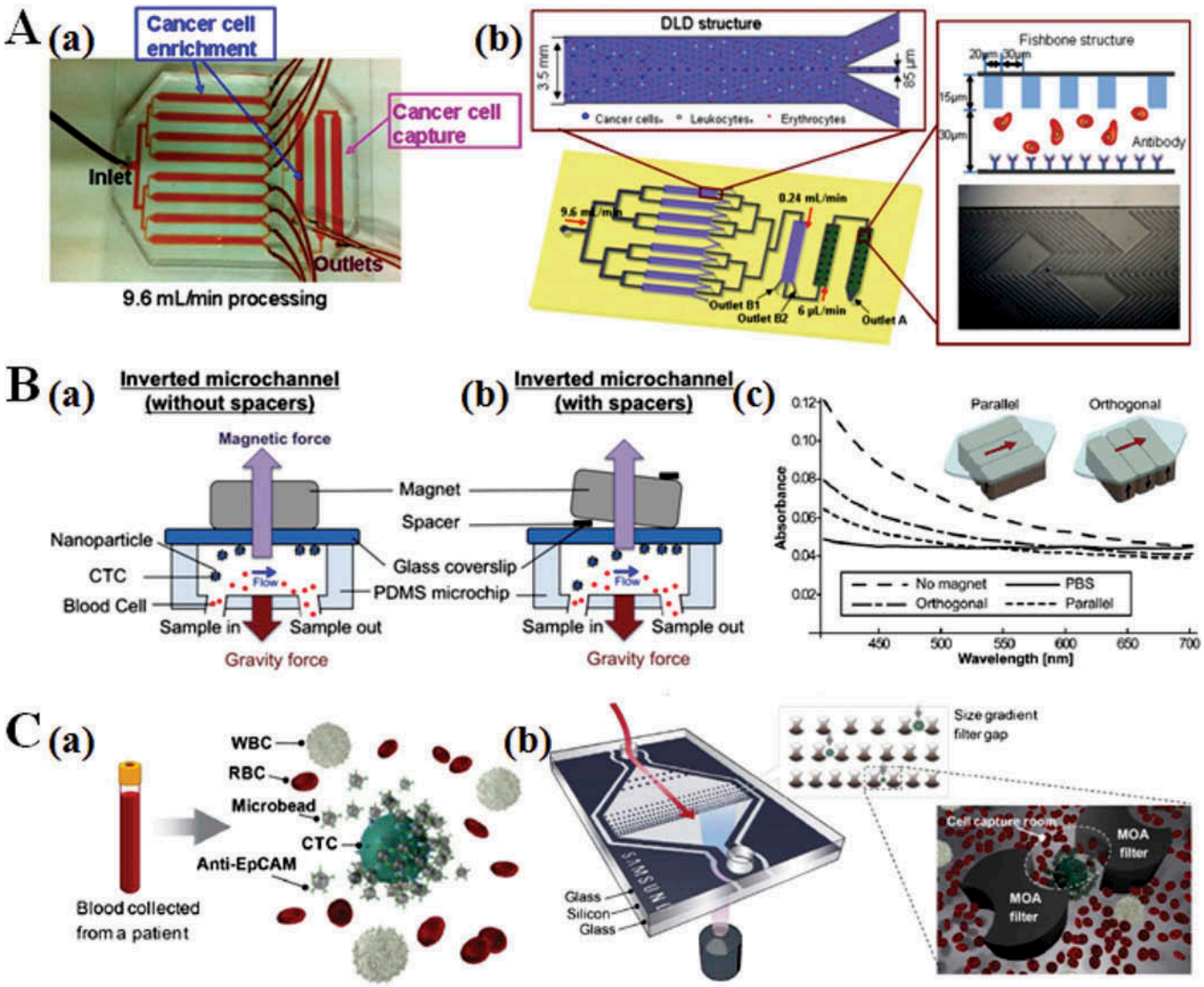

FIGURE 5 Immunoaffinity-based microfluidic systems for the positive selection of CTCs. (A) EpCAM antibody–coated microfluidic channel system for cancer cells enrichment and capture. (a) Device design. (b) Cancer cell enrichment and capture principle. Microfluidic deterministic lateral displacement (DLD) chamber with mirrored triangular micropost array. Capture chamber with anti-EpCAM modified substrate and overlaid PDMS layer with fishbone structure for cancer cell capture. Adapted from Ref. (75); (B) Microfluidic design of magnet-guided immunomagnetic-based cell separation. (a) Principle of operation of the inverted microchip. Magnetic bead-labeled CTCs are captured to the microchannel substrate by the magnetic field as the blood sample flows through the microchannel. Gravity force drags blood cells to the opposite side of the microchannel substrate. (b) A spacer, placed between the magnets and microchannel, is introduced to create magnetic field gradient increasing throughout the whole microchannel. (c) Control screening experiment with only magnetic beads in buffer solution in the flow channel. Optical transmission is measured for orthogonal and parallel arrangements of magnets, with the parallel arrangement being best. Adapted from Refs. (84, 85); (C) Microfluidic design of size-amplified immunomagnetic-based cell separation. (a) Selective size amplification using magnetic microbeads conjugated with anti-EpCAM. (b) Multi-obstacle architecture (MOA) size-gradient filter chip. The MOA filter unit has two filter gaps, and jamming of cells is mitigated by a "cell capture room" between the first and second filter gaps. Adapted from Ref. (51).

tumor cells and endow them with appropriate magnetism for the next magnetic separation by magnets (Figure 5B) (84, 85, 92–94). The other is to bind tumor cells surface and thus increase the cells dimensions, and this selective size amplification of tumor cells will allow the next size-based separation to achieve higher recovery and purity rates than conventional filtration methods (Figure 5C) (51, 95–97). Correspondingly, various filter designs, such as multi-obstacle architecture (MOA) (51) and tracheal carina-inspired bifurcated (TRAB) filter (97), have been developed for capturing size-amplified CTCs. However, these immunomagnetic cell separation techniques generally require pretreatment of the samples with the magnetic beads that coated with specific antibodies.

Negative Selection. Although positive selection methods can be used to separate CTCs at a high purity, these kinds of methods may have potentially significant limitations, one of which is that CTCs, heterogeneous by nature, do not all express the same or the same level of specific antigens. Even with the same origin cancer cell lines, the surface densities of epitopes are quite distinct from each other. The biological characteristics of the tumor cells, after antibody-antigen reactions *via* positive selection methods, may also be affected. In addition, positive selection of CTCs requires an assumption about the unknown nature of CTCs in the blood sample. For these reasons, negative selection methods, in which the blood sample is depleted of leukocytes using antibodies against CD45 and other leukocyte antigens (which are not expressed on the tumor cells surface), are growing in popularity for the collection of CTCs (98).

Same as the positive selection, negative selection can be also realized by either modifying microchannel substrate surface with antibodies or manipulating antibodies-conjugated micrometer-sized magnetic beads (Table 1). The former type of negative selection methods is commonly performed by CD45 antibodies-immobilized microfluidic channels. To increase the surface interactions between the nontarget leukocytes and the channel surface, the roughened microchannel systems are generally created by conventional lithography techniques (99) or using strong acid (Figure 6A) (100). The latter type of immunomagnetic beads–based negative selection methods can be performed in many forms for collecting CTCs, such as multistage concentric-circular magnet on microfluidic disk (101), fluorescent-activated cell sorting (102), and microslit membrane (103, 104). The most promising one is the so-called CTC-iChip technology using two-stage magnetophoresis and depletion antibodies against leukocytes (Figure 6B). This CTC-iChip that integrates DLD, inertial focusing and magnetophoresis can sort up to 10^7 cells/s and successfully collect CTCs from the whole blood of both epithelial and nonepithelial cancer patients including lung, prostate, pancreas, breast and melanoma (93, 105). However, it should be noted that not all CD45-negative cells in the blood are tumor cells (for example, the circulating endothelial cells) (26). Therefore, subsequent characterization and detection steps are of utmost importance to increase the specificity and accuracy of these negative selection-based microfluidic systems.

Separation and Analysis of Exosome

Exosomes, carrying cell-specific cargos (proteins, lipids and nucleic acids) and distributing ubiquitously in body fluids, can be harnessed as a minimally invasive means to probe the tumor origin and progression status. Although a number of recent studies have highlighted the potential clinical role of exosomes in disease diagnosis and therapy (10), routine exosome analysis is still a challenging task. Compared to conventional exosome separation techniques, such as ultracentrifugation, density gradient and physical force (126), microfluidics provide great opportunities for exosome analysis in terms of reagent volumes, automation and integration capabilities, separation time, product integrity and purity, and recovery rate (127). Generally, vesicle size (20–300 nm) and surface biomarkers (such as EpCAM, CD9, CD63 and CD81) are two typical characters to identify exosomes. Therefore, current reported microfluidic

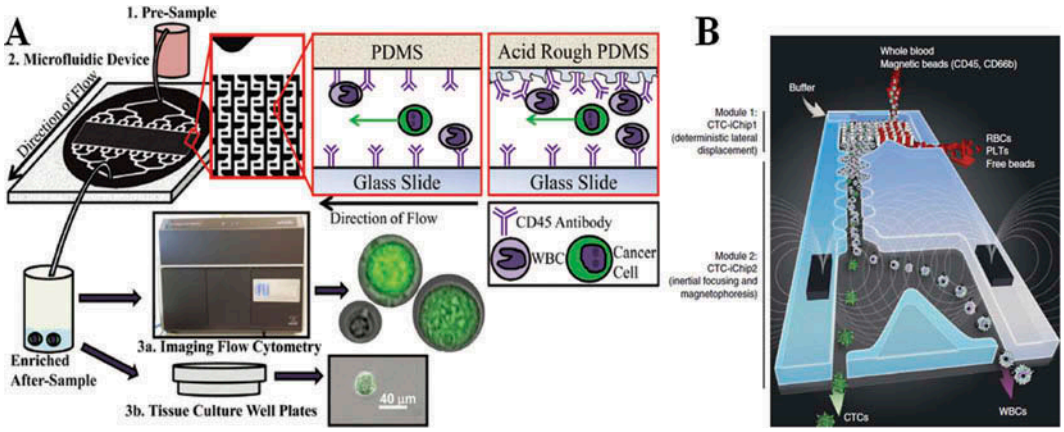

FIGURE 6 Immunoaffinity-based microfluidic systems for the negative selection of CTCs. (A) Experimental design of CD45 antibodies–immobilized microfluidic system: (1, 2) blood pre-samples with spiked cancer cells are injected through the depletion device functionalized with anti-CD45 antibody to specifically bind to white blood cells (WBCs). Eluted cells comprising the target CD45-cells and false-positive WBCs are collected and characterized using either imaging flow cytometry (3a) or optical microscopy after plating in standard tissue culture wells (3b). Adapted from Ref. (100); (B) Immunomagnetic-based CTC-iChip schematic. The CTC-iChip is composed of two separate microfluidic devices that house three different microfluidic components engineered for inline operation: DLD to remove nucleated cells from whole blood by size-based deflection by using a specially designed array of posts performed in CTC-iChip1, inertial focusing to line up cells to prepare for precise magnetic separation and magnetophoresis for sensitive separation of immunobeads-labeled WBCs and unlabeled CTCs, which are performed in CTC-iChip2. Adapted from Reference (105).

systems for exosome separation and analysis can be simply classified into two categories: size-based analysis and immunoaffinity-based analysis (Table 2).

Size-based separation and analysis

Size-based microfluidic systems for exosome analysis are generally established on the basis of nanoporous structure (128–131). One typical example is the so-called ciliated micropillar structure array that is formed by the electrolessly etching on the silver eletrodeposited sidewalls of micropillars (Figure 7A) (128). The inner-nanowire spacing can be tuned within a size range of 30–200 nm to create a high density of interstitial sites, which allows physical trap of exosomes. The micropillars not only provide walls for anchoring the nanowires but also filter larger-sized sample components and function as the structural supports for the microfluidic channel. This nanowire-on-micropillar hierarchical structure showed fast trapping rate, specific selection and high retention rate toward exosome vesicles. Similar nanoporous structures or arrays can be also seen in other microfluidic filtration system to separate exosomes with tunable size cut-off (129–131). However, these physical trapping approaches may be restricted by the saturation limit. Alternatively, an acoustic nanofilter microfluidic system was developed for separating the exosomes in a size-specific, continuous and contact-free manner (Figure 7B) (132). The separation uses ultrasound standing waves to exert differential acoustic force on exosomes according to their size and density. By optimizing the design of the ultrasound transducers and underlying electronics, a high separation yield and resolution can be achieved. And the "filter size cutoff" can be controlled electronically in situ, which enables versatile extracellular vesicles-size selection (Figure 7B). Another interesting approach for the separation and titration of exosomes is the colorimetric nanoplasmonic assay, which can achieve naked eye readout and femtomolar detection (133). Table 2 summarizes the separation and analysis of size-based microfluidic systems for exosomes. It is noted that although size is the most acceptable criterion for exosome identification, it is not a strict feature of exosomes. Therefore, it is crucial to design novel microfluidic methods that can combine multiple features for separating and characterizing vesicle types and allowing precise analysis of respective exosome functions.

Immunoaffinity-based separation and analysis

Immunoaffinity-based microfluidic systems for exosome analysis can be implemented by either modifying microchannel substrate surface with antibodies (8, 134–140) or manipulating antibodies-conjugated micrometer-sized beads (141–143). The former type of microfluidic systems was first reported in 2010 using an anti-CD63 functionalized microchannel surface for immunocapture of exosomes (136). Since then, different kinds of microfluidic devices modifying with specific antibodies toward exosome surface biomarkers were designed (Table 2). Among these, a typical example is the nanoplasmonic exosome (nPLEX) microfluidic system, which is based on transmission surface plasmon resonance through periodic nanohole arrays (Figure 8A) (8). Each array surface is functionalized with affinity antibodies for different exosome protein markers, such as CD9, CD63, HSP70, HSP90, Flotillin 1, Flotillin 2, CD24 and EpCAM. With target-specific exosome binding, the nPLEX microfluidic system displays spectral shifts or intensity changes proportional to target marker protein levels. Therefore, this nPLEX technology enables high-sensitive and high-throughput monitoring of exosome binding in real-time and with single-exosome resolution (Figure 8A).

Although various microchannel surface modification approaches were configured to enhance the capture efficiency of exosomes, the capture capacity was still limited by available surface area for antibodies immobilization. Therefore, micrometer-sized immunobeads were generally introduced into microfluidic systems to enhance the capture capacity of exosomes (Table 2). One kind of immunobeads reported in previous studies was based on polystyrene particles (142). There, inertial lift forces push the polystyrene beads toward the center of microfluidic channel with multiple outlets, transferring them into a wash buffer and allowing their selective separation. Comparatively, magnetic particles-based immunobeads bring many superior features, especially their easy manipulation by an external magnetic force (82, 83, 141, 143). Specifically, when the immunomagnetic beads were mixed with exosomes, the bound complex can be retained as a tight aggregate in the downstream microfluidic chamber by magnetic force. The amount of the retained beads was proportional to the injection volume of exosomes, thus allowing for quantitative separation and analysis (Figure 8B). Compared to the microchannel substrate surface modification-based immunoaffinity analysis, the immunobeads method allows for rapid enrichment of captured exosomes and convenient sample preparation for following characterization in addition to higher capture efficiency and analysis sensitivity due to the larger surface area. However, premixing and incubation of immunobeads with exosome samples are needed.

Separation and Analysis of cNAs

Nucleic acid analysis could enhance the understanding of biological processes and disease progression, elucidate the association of genetic variants and disease, and lead to the point-of-care design and implementation of new treatment strategies (21). Conventional methods for separation and analysis of cNAs in liquid biopsy have some limitations in that they are labor-intensive and high cost, and exhibit unavoidable sample loss in the multistep treatment. Thus, microfluidic systems can provide researchers with a promising alternative tool to validate these circulating biomarkers.

TABLE 2
Microfluidics-based separation and analysis of exosomes

Sample type	*Size*	*Biomarker type*	*Microfluidic forms*	*Separation methods*	*Flow rate/volume/time*	*Detection limit/ recovery rate*	*Reference and year*
Size-based separation and analysis							
Mouse whole blood	~150 nm	CD9	PMMA integrated with PPM	Pressure; EP	*Pressure*:1 μL/min; 40 min. *EP*: 2 μL/min; 240 μL; 2 h	1.5%	(129) 2012
Mixture of BSA, liposomes, and PS beads	83–120 nm		PDMS/Silicon with concentric radial channel	Ciliated micropillar array	10 μL/min; 10 min	10–60%	(128) 2013
BxPC-3	<220 nm		PDMS/Silicon with obstacle array	DLD	200 μL	39%	(130) 2014
Murine embryonic stem cell line (D3)	~100 nm		PDMS/Glass with parallel channels	Pressure	6.5 μL/min	>80%	(131) 2014
OvCA429	<200 nm	CD63; HSP90; HSP70; Flotillin-1	PDMS/Silicon with SSAW	Acoustic	50 μL	>90%	(132) 2015
Immunoaffinity-based separation and analysis							
Whole blood from glioblastoma patient	~100 nm	CD63	PDMS with a straight flow channel	Antibody microchannel	16 μL/min; 10–400 μL	42–94%	(136) 2010
SKMG3; GBM20/3; GLI36vIII	50-150 nm	CD63	PDMS/Glass with μNMR-integrated platform	Immunomagnetic beads		>90%; 10^4 vesicles	(144) 2012
Whole blood	<200 nm	CD44; CD47; CD55	PDMS/Glass with μNMR-integrated platform	Immunomagnetic beads	150 μL; <30 min	~2×10^6 vesicles/μL	(145) 2013
MHCC97L; MHCC97H; B16-F1; B16-F10	~70 nm	CD9; CD63; CD41b; CD81; CD82; E-cadherin; EpCAM	PlexArray Nanocapture Sensor Chip	SPRi antibody microarray	5 μL/s and 5 μg/mL	~4.87×10^7 exosomes/ cm^2	(134) 2014
Human ovarian carcinoma cell lines; Ascites from ovarian cancer patient	~100 nm	CD9; CD63; HSP70; HSP90; Flotillin 1; Flotillin 2; CD24; EpCAM	PDMS/Silicon with parallel channels	nPLEX assay	*CCS*: 0.2–2 μL/min; *Ascites*: 10 μL/min; 15 min	2–3%	(8) 2014
Whole blood from pancreatic cancer patient	30–300 nm	CD63	PDMS/Glass with eight circular chambers	ExoChip assay	8 μL/min; 400 μL		(137) 2014
BT-474; MDA-MB-231; PC3	30–350 nm	CD9	PDMS/Silicon with parallel microchannels	ac-EHD induced nanoshearing	2 h	2760 exosomes/ μL	(139) 2014
Plasma from NSCLC patient	40–150 nm	EpCAM; CA-125; α-IGF-1R; CD9; CD63; CD81	PDMS/Glass with a cascading microchannel network	Immunomagnetic beads	30 μL; 100 min	>99.9%	(143) 2014
Melanoma cell; breast cancer cell	~75.4 nm	CD63; EpCAM	PDMS/Glass with RInSE microchannel	PS beads	70 μL/min	~100%	(142) 2015
SKMG3; GLI36vIII	50–200 nm	CD63	PDMS/Glass with iMER-integrated platform	Immunomagnetic beads	~100 μL; <2 h	>93%	(140) 2015
Plasma from ovarian cancer patient	<150 nm	CA-125; EpCAM; CD24	PDMS/Glass with a Y-type channel	Immunomagnetic beads	20 μL; 20 min	72%	(141) 2016
Plasma from ovarian cancer patient	<150 nm	CD9; CD63; CD81; EpCAM	PDMS/Glass with Y-type microposts	Nano-IMEX with GO and PDA	2 μL	80 aM	(138) 2016
MCF-7; MDA-MB-231		CD9; CD63; CD81	PDMS/Silicon with through-hole mesh	PDMS mesh		3%	(135) 2016

ac-EHD: Alternating current electrohydrodynamic; BSA: Bovine serum albumin; CCS: Cell culture supernatant; EP: Electrophoresis; DLD: Deterministic lateral displacement; GBM: Glioblastoma multiforme; GO: Graphene oxide; iMER: Immunomagnetic exosomal RNA; IMEX: Interfaced microfluidic exosome; nPLEX: Nano-plasmonic exosome; NSCLC: Nonsmall-cell lung cancer; PDA: Polydopamine; PDMS: Polydimethylsiloxane; PMMA: Poly(methyl methacrylate); PPM: Porous polymer monoliths; PS: Polystyrene; RInSE: Rapid inertial solution exchange; SSAW: Standing surface acoustic wave.

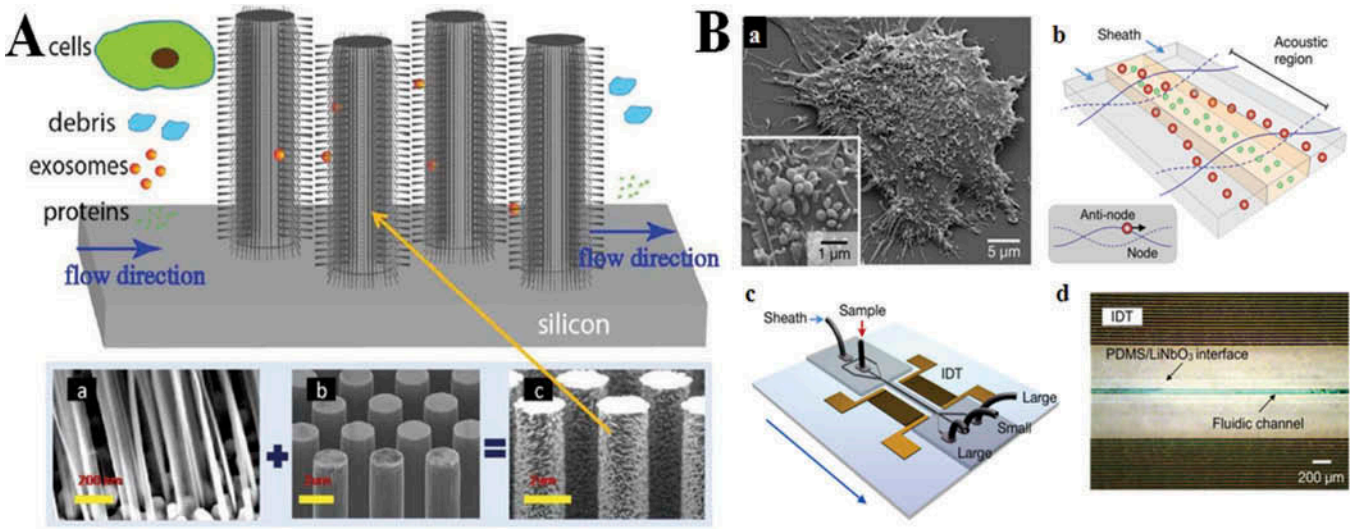

FIGURE 7 Size-based microfluidic systems for exosome analysis. (A) A schematic of the ciliated micropillar array for exosome separation. The cells are depleted before entering the micropillar region, while cellular debris as well as proteins and other small objects flow through, bypassing the micropillars. Exosomes are highly enriched by trapping within the nanowires. Inset (a): representative porous silicon nanowire forest. Inset (b): micropillars. Inset (c): representative ciliated micropillars. Adapted from Ref. (128); (B) Acoustic nanofilter for label separation of exosomes. (a) SEM image of cell released microvesicles. (b) Filter operation. Microvesicles in the acoustic region are under the acoustic radiation pressure and transported to nodes of acoustic pressure region (inset). Larger vesicles move faster as the acoustic force is proportional to the vesicle volume. Sheath flows, positioned at the node region, remove large vesicles, whereas the center flow retains small vesicles. (c) Device schematic. A pair of interdigitated transducer (IDT) electrodes is used to generate a standing surface acoustic wave across the flow direction. Large microvesicles are collected at the two side outlets, and small vesicles at the center outlet. (d) Micrographs of a prototype device. The IDT electrodes were patterned on a piezoelectric ($LiNO_3$) substrate. The fluidic channel was permanently bonded to the substrate. Adapted from Ref. (132).

Electrophoretic and fluorescent dyes labeling techniques are predominantly conducted in the analysis of nucleic acids. The first widespread technique for controlling the liquid flow and the first microfluidic device employed electric fields to pump fluids (23). This system can also be used to separate ionic nucleic acids species, especially with the addition of linear polymers for achieving the desired resolution (146). In addition, the transparency of glass and polymer (such as PDMS) substrates also allows cNAs species to be detected fluorescently (20). Because DNA molecules can be ratiometrically labeled with fluorescent intercalating dyes and detected with high signal-to-noise ratio, most nucleic acid analysis methods rely on fluorescence-based instruments, such as confocal microscope and fluorescent microscope. In recent years, microfluidic-based separation of nucleic acids molecules was realized by many different ways, such as the regulation of fluid shear flow force, electronic field, magnetic field, organic solvents, specific surface modifications, the addition of polymer, the size of nucleic acids themselves, the formation of droplets and the use of micro-/nano-structured arrays (Table 3) (17, 21, 147). However, processing of the reaction products is typically not done in conventional microfluidic systems, and post-reaction processing, such as qPCR, digital PCR and sequencing, is widely used in separation systems. While PCR methods are highly sensitive and used near exclusively, they have intrinsic limitations, such as amplification errors, reproducibility and varying amplification efficiencies.

This situation boosts the design and fabrication of more powerful integrated and streamlined microfluidic devices. Practically, one of the main advantages of microfluidic systems is that many different techniques can be combined within a single device, which allows us to perform many sequential operations, such as sample preparation, reaction, separation, purification and analysis (148, 149). One of the first highly integrated DNA microfluidic analysis systems was developed in 1998 (Figure 9A) (150). This device is capable of measuring nanoliter DNA samples, mixing the solutions together, amplifying or digesting the DNA to form discrete products, and separating and detecting those products. As an emerging and powerful tool in integrated microfluidic systems, gene microarray chips that are fabricated by photolithography or spotting method also hold great promise for real-time and high-throughput analysis (23). Another typical integrated system is the so-called microfluidic cylindrical illumination confocal spectroscopy (μCICS), which was developed as a one-step assay for analyzing circulating DNA size and quantity directly in human serum (Figure 9B) (20). Obviously, integrating components into a single system significantly increases the difficulty of system design and operation compared with conventional single-component systems. Therefore, even

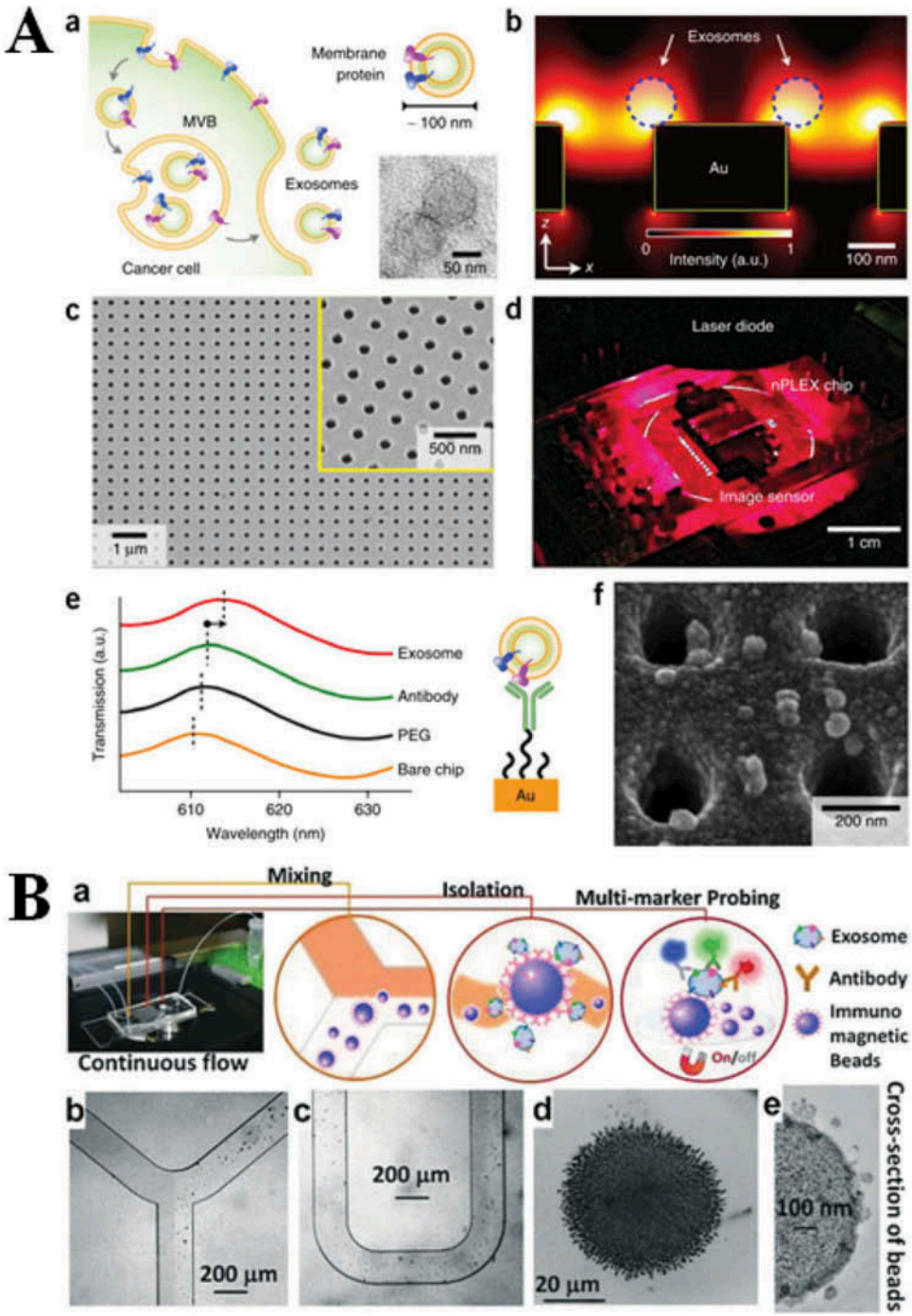

FIGURE 8 Immunoaffinity-based microfluidic systems for exosome analysis. (A) Surface modification of antibodies on plasmonic substrate for microfluidic-based exosome analysis. (a) Cancer cells secrete an abundance of exosomes through fusion of a multivesicular body (MVB) with the cellular plasma membrane. The inset TEM image shows exosomes from CaOV3 cell. (b) Finite-difference time-domain simulation shows the enhanced electromagnetic fields tightly confined near a periodic nanohole surface. The field distribution overlaps with the size of exosomes captured onto the sensing surface, maximizing exosome detection sensitivity. (c) A SEM image of the periodic nanoholes in the nanoplasmonic exosome (nPLEX) sensor. (d) A prototype miniaturized nPLEX imaging system developed for multiplexed and high-throughput analyses of exosomes. (e) A representative schematic of changes in transmission spectra showing exosome detection with nPLEX. The gold surface is pre-functionalized by a layer of polyethylene glycol (PEG), and antibody conjugation and specific exosome binding were monitored by transmission spectral shifts as measured by nPLEX. (f) SEM image shows exosome capture by functionalized nPLEX. Adapted from Ref. (8); (B) Surface modification of antibodies on micrometer-sized beads for microfluidic-based exosome analysis. (a) Workflow of the ExoSearch chip for continuous mixing, separation and in situ, multiplexed detection of circulating exosomes. (b, c) Bright-field microscope images of immunomagnetic beads manipulated in the microfluidic channel for mixing and separation of exosomes. (d) Exosome-bound immunomagnetic beads aggregated in the microchamber with an on/off switchable magnet for continuous collection and release of exosomes. (e) TEM image of an exosome-bound immunomagnetic bead in a cross-sectional view. Adapted from Ref. (141).

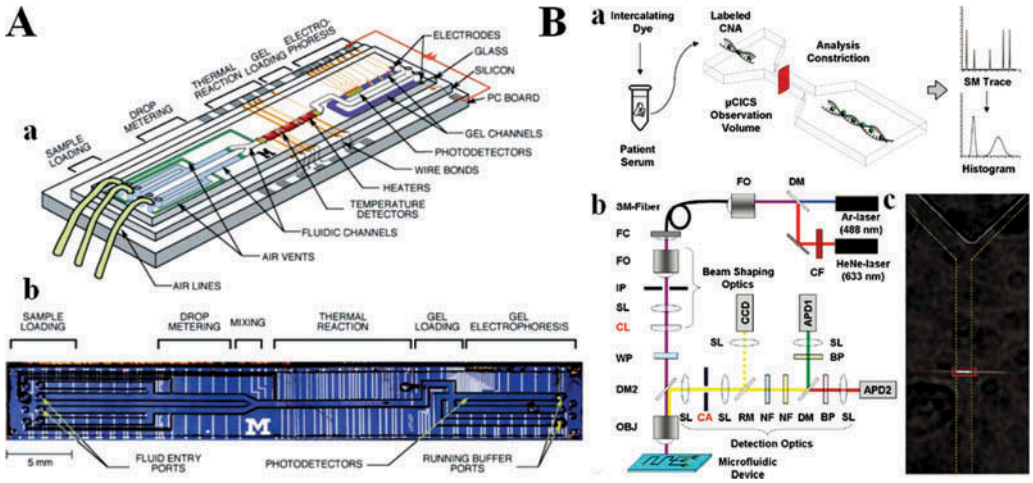

FIGURE 9 Integrated microfluidic devices for nucleic acids analysis. (A) An integrated nanoliter DNA microfluidic analysis device. (a) Schematic of integrated device with two liquid samples and electrophoresis gel present. Color code: blue, liquid sample (ready for metering); green, hydrophobic surfaces; purple, polyacrylamide gel. (b) Optical micrograph of the device from above. Wire bonds to the printed circuit board can be seen along the top edge of the device. Adapted from Ref. (150); (B) An integrated microfluidic cylindrical illumination confocal spectroscopy (μCICS) system for circulating nucleic acids detection. (a) Schematic illustration of the one-step, PCR-free, single-molecule DNA sizing assay. (b) Optical component diagram of μCICS platform. (c) CCD image of the μCICS illumination sheet focused into the microfluidic analysis constriction. The channel boundaries are demarcated by dashed yellow lines, while the projection of the confocal aperture into sample space is shown in red. Adapted from Ref. (20).

though such devices are theoretically possible, the commercialization and widespread development of these fully integrated and automated systems are still largely demanded in the future. However, the availability of robust microfabrication techniques and high unit demand should facilitate the development of "Sample-In, Answer-Out" point-of-care nucleic acids analysis platform and thus utilize them to benefit our humankinds. Examples of microfluidics-based separation and analysis of nucleic acids are summarized in Table 3.

CURRENT CHALLENGES AND FUTURE PERSPECTIVES

CTCs

The rare and heterogeneous properties of CTCs are still two significant facts to be drawn from the liquid biopsy approaches. Given the significance of CTCs in the metastatic process and the potential roles of using these cells for noninvasive cancer theranostics, great efforts have been made to develop robust CTCs separation and analysis approaches. Many emerging and scalable microfluidic systems, including our own, demonstrated feasibility under clinical settings for separating CTCs at increasingly higher yields and facilitate downstream analyses. The current progress of these microfluidic systems for CTCs separation and detection is summarized, and the working principles and experimental results of key microfluidic technologies are tabulated above (Figure 2 and Table 1). These microfluidic systems are generally based on label-free techniques (including hydrophoresis and dielectrophoresis strategies) and immunoaffinity techniques (including positive selection and negative selection strategies) (Figure 2). Despite the recent technological advances, the development of a single portable device capable of simultaneously achieving short processing time, high CTCs recovery and high throughput remains challenging.

For label free-based microfluidic techniques, both hydrophoresis and dielectrophoresis strategies relying on the physical properties of cells can have a high throughput as these strategies are well compatible with high cell flow rates. Hydrophoresis strategies can also enable high capture rates of CTCs due to the actual size and deformability differences between CTCs and hematological cells. However, these hydrophoresis strategies, especially filtration methods, may suffer from the cell viability issue resulting from potential damage incurred when the cells pass through the obstacle arrays in a narrow passage. In addition, size overlapping between CTCs and WBCs also indicates that any size-based separation strategies may lead to a loss of relatively small-sized CTCs (Figure 3A). Dielectrophoresis strategies, which can leverage differences in the size and electric properties of cells, hold a great promise to lead to high CTCs capture efficiency compared to the hydrophoresis strategies that are generally based on the cells size differences only. However, because of the limited electric differences between target cells and background

TABLE 3
Microfluidics-based separation and analysis of nucleic acids (NAs)

NAs type	*Sample type*	*Microfluidic forms*	*Separation methods*	*Volume/time*	*Analysis tools*	*Detection range/ limit/efficiency*	*Reference and year*
DNA	*Mycobacterium tuberculosis*	Silicon/glass with Y-type channel	EP	120 nL; 15 min	PAGE	0.12 mg/mL	(150) 1998
DNA	λ-phage	Glass/Silicon with taper shape array	DLA (Stretching)		Confocal microscope	120 μg/mL	(151) 2004
DNA	λ-phage; T2-phage; Whole blood	PDMS/Silicon with parallel millimeters channels	EP	Microliter	AILIIM	25 μg/mL	(152) 2004
DNA	λ-phage	PCB with multilayer set of coils	Magnetic droplet manipulation system	~10 μL	PCR; AGE	1.25 μg/mL	(153) 2006
miRNA	IDT	Microfluidic capillary	LNA-DNA	1 fL	Confocal microscope	500 fM	(154) 2006
mRNA	NIH/3T3 cells	PDMS/glass with multilayer channels	Magnetic Dynabeads™ with oligo(dT)$_{25}$	4 nL	qRT-PCR	0.3–100 pg	(155) 2006
DNA	*B. subtilis; S. aureus; E. coli*	96-well SPRI reactor plate with LAMIs	Gradient micropillar array	~1 μL	AGE	~10 ng	(156) 2008
miRNA	Plasma from prostate cancer patient	TaqMan™ miRNA microarray	mirVana™ PARIS™ Kit	2 μL	qRT-PCR	100% sensitivity	(157) 2008
DNA	λ-phage; T2-phage	PDMS/Glass with parallel channels	Oscillatory shear flow (Stretching)		AILIIM	100% sensitivity	(158) 2009
mRNA	*C. parvum* oocysts	PMMA/Glass with a sawtooth channel	Magnetic Dynabeads™ with oligo(dT)$_{25}$	3.5 μL	Fluorescent microscope	From 5 oocysts	(159) 2009
DNA	IDT	PDMS/Glass with multilayer channels	MB	0.1 μL; <30 min	Confocal microscope	5 pM	(160) 2009
DNA	Serum from lung cancer patient	PDMS with Y-type channel	None	<10 pL; 10 s	μCICS	100% mass detection efficiency	(20) 2010
DNA	λ-phage	PMMA/Silicon with micropillar array	None	3 μL	EOM; SEM	1×10^{-18} M	(161) 2011
DNA	Cell lines bearing *KRAS* alleles	PDMS/Silicon with droplets-forming channels	None	Picoliter	Confocal microscope	1/200000	(162) 2011
DNA;RNA	IDT	PDMS/Glass with a ring-shape channel	None	Picoliter	Confocal microscope	100 pM	(163) 2011
DNA; rRNA	Whole blood from ovarian cancer patient	PDMS/Silicon with a V-shape droplets-forming channels	SPE	5 μL	AGE		(164) 2011
DNA	BAC	Glass/Silicon with micropillar array and parallel channels	Gradient micropillar array (Stretching)		Fluorescent microscope	5 μg/mL	(165) 2012
DNA	λ-phage	PDMS/glass with cross slots	PEG-NaCl (Stretching)		Fluorescent microscope	1 pM	(166) 2012
DNA	λ-phage	PeT microchip by direct-printing	EP with polymer	1.5 nL; 4 min	Bioanalyzer™ 2100	25 μg/mL	(146) 2012
miRNA	Whole blood from breast cancer patient	Geniom™ Biochip miRNA microarray	miRNeasy™ kit		Bioanalyzer™ 2100	85.6% detection accuracy	(167) 2012
miRNA	HEK293 cells	Gold microelectrodes array	Electrochemistry	Picoliter	Potentiometry	20 pM	(168) 2012
RNA	IDT	Glass with droplets-forming crossed-channel	Agarose	Picoliter	Flow cytometry; Fluorescent microscope	100% sensitivity	(169) 2012
rRNA	*E. coli*	PDMS/Silicon with droplets-forming channels	PNA	Picoliter	Confocal microscope	1.56 nM	(170) 2012
DNA	Whole blood from CLL patient	100 sites NanoChip™ with checkerboard pattern	DEP	20 μL	Fluorescent microscope	8–16 ng/mL	(171) 2013
mRNA	*C. parvum* oocysts	PMMA with parallel channels	PAMAM dendrimer		NASBA; LFA	From 30 oocysts	(172) 2014
DNA	saliva/plasma from lung cancer patient	GeneFluidics™ chip with 16 bare gold electrode	Electrochemistry	20–40 μL; <10 min	FISH	1/1000	(173) 2014

(*Continued*)

TABLE 3
(Continued)

NAs type	*Sample type*	*Microfluidic forms*	*Separation methods*	*Volume/time*	*Analysis tools*	*Detection range/ limit/efficiency*	*Reference and year*
DNA	λ-phage; Whole blood	100 sites NanoChip™ with checkerboard pattern	DEP	15 min	Epifluorescent microscope	200 pg/mL	(174) 2014
mRNA	GBM cell lines; Whole blood from GBM patient	PDMS/Glass with iMER-integrated platform	Glass beads filter	~100 μL; 2 h	qRT-PCR	90%	(140) 2015
miRNA	PANC1 cells	Plastic/$LiNbO_3$ with Ti/Al electrode	SAW	~100 μL; 1.5 h	Ion-exchange nanomembrane	2 pM	(175) 2015
DNA	Whole blood	PDMS/PMMA with a U-shape	QIAamp™ kit	1 μL	Magnetoresistive sensor	0.6 μM	(176) 2016

μCICS: Microfluidic cylindrical illumination confocal spectroscopy; AGE: Agarose gel electrophoresis; AILIIM: Argon ion laser-illuminated inverted microscope; BAC: Bacterial artificial chromosome; CLL: Chronic lymphocytic leukemia; DEP: Dielectrophoresis; DLA: Direct linear analysis; EOM: Epifluorescence optical microscopy; EP: Electrophoresis; FISH: Fluorescence *in situ* hybridization; GBM: Glioblastoma multiforme; IDT: Integrated DNA technology; iMER: Immunomagnetic exosomal RNA; LAMIs: Large area mold inserts; LFA: Lateral flow assay; LNA: Locked nucleic acid; MB: Molecular beacon; miRNA: MicroRNA; mRNA: Messenger RNA; NASBA: Nucleic acid sequence-based amplification; PAGE: Polyacrylamide gel electrophoresis; PAMAM: Polyamidoamine; PCB: Printed circuit board; PCR: Polymerase chain reaction; PDMS: Polydimethylsiloxane; PEG: Polyethylene glycol; PeT: Polyester-toner; PMMA: Poly(methyl methacrylate); PNA: Peptide nucleic acid; qRT-PCR: Quantitative reverse transcription polymerase chain reaction; rRNA: Ribosomal RNA; SAW: Surface acoustic wave; SEM: Scanning electron microscopy; SPE: Solid phase extraction; SPRI: Solid-phase reversible immobilization.

cells, these dielectrophoresis strategies are still not getting as high yield performance as expected.

For immunoaffinity-based microfluidic techniques, there are two types of approaches for capturing and collecting CTCs, *i.e.*, positive selections and negative selections. Both of them can be generally realized by either modifying microchannel substrate surface with antibodies or manipulating antibodies-conjugated micrometer-sized magnetic beads. A significant challenge in the antibodies-immobilized microchannel methods for both positive selections and negative selections is their relatively low processing throughput. This situation is caused by a limited number of interaction sites between the surface-bound ligands and the target cells. The possibility of nonspecific capture also makes it more complicated. Specifically, cell flow rates need to be slow enough to ensure the maximum target cells retention, but reasonably fast enough to generate shear force to prevent nonspecific attachment of nontarget cells to the channel surface. Therefore, although various microchannel structures have been developed to show increased performance, microfluidic devices with high CTCs recovery rate, purity and throughput still remain to be achieved. Regarding the immunomagnetic beads methods for CTCs separation, the heterogeneous property of tumor cells that may not express the same or the same level of specific antigens makes the negative selections much more appealing than the positive selections. Negative selections not only enable the simultaneous separation of various types of CTCs but also allow the target cells to be collected in an intact form.

Despite great efforts have been achieved, many works still need to be done for further improving the separation efficiency and analysis sensitivity of CTCs in microfluidic systems. The well-developed versatile microfabrication techniques can provide new ideas in the design and construction of microfluidic channels, which will be greatly helpful for target cells captured inside microchannels. Current advances of nanobiotechnology can also be used in this field, especially for immunomagnetic beads-based cells separation. For example, many studies shed light on the important roles of shape and surface chemistry of micro-/nano-particles on biological effects, such as cell binding kinetics, margination in laminar flows, surface functionalization density of ligands and even cell toxicity (177, 178). These will bring new insights for the design of immunomagnetic beads to achieve short processing time and high CTCs recovery rate. Another approach that utilizes a combination of multiple cell capture techniques may provide tremendous opportunities for improving the CTCs capture performance of microfluidic systems. We can envision a multi-module microfluidic system for CTCs capture in which some modules perform high throughput concentration and purification of tumor cells, while some others enable the selective capture of specific tumor cells. The prototypes of such kinds of devices can be found in recent studies, which may guide the focus of future research (51, 75, 105). In addition, it is noteworthy that most of current tests in microfluidic systems were carried out using spiked samples (spiking tumor cells into PBS, cell culture medium or whole blood from healthy individuals) rather than real clinical samples from cancer patients (Table 1). Because of the complexity of the peripheral blood and tumor microenvironment of cancer patients, such tests may not properly reflect the effectiveness of microfluidic devices, and may thus hinder their research and development.

Exosome

Tumor-derived exosome as a promising alternative in liquid biopsy offers new clinical opportunities for minimally invasive diagnostics and monitoring of cancer diseases. The separation and analysis capabilities of exosomes in microfluidic systems are summarized in Table 2, which shows their superior performance compared to that of conventional techniques, such as ultracentrifugation and commercial kits. Such improvements in terms of response time, sensitivity and selectivity from microfluidic systems will greatly enhance the specific role of exosome in existing circulating tumor biomarkers and address current hurdles in liquid biopsy of cancers. However, exosome secretion is a dynamic process, producing diverse populations with large differences in size and concentration. Exosomes, during the treatment process, also suffer from the stability issue (179). Therefore, precise measurement and analysis of exosomes are still quite challenging.

Current established microfluidic systems for exosomes separation are generally based on either size or immunoaffinity techniques. The performance of size-based exosome separation techniques will certainly be affected by the population size differences as mentioned above. In this situation, it is important to determine the design of microfluidic devices in order to avoid passage clogging and exosome vesicle trapping issues. In addition, because the sizes of exosomes are in the nanometer range and thus much smaller than the sizes in conventional microfabrication technologies, more advanced technologies are still required to achieve high yield and purity of exosomes for clinical translation. To this end, a novel multidimensional hierarchical structure (termed “ciliated nanowire-on-micropillar”) with a combination of silicon microfabrication processes, electroplating and electroless metal-assisted nanowire etching techniques was developed in our laboratory (128). Comparatively, immunoaffinity-based exosome separation techniques can lead to relatively high specificity and rapid analysis. However, significant challenges still exist in this field, for both antibody-immobilized microchannel methods and immunobeads methods. For example, there is currently no “ubiquitous” biomarker to distinguish subsets of exosomes from each other, due to the fact that exosomes also have a heterogeneous nature similar to CTCs. Therefore, there are very limited biomarkers that can accurately distinguish cancer-specific exosomes from normal exosomes.

To date, efficient and reliable microfluidic systems for the separation of circulating tumor exosomes are still lacking, which lead to the exosomes-related research far lagging behind than CTCs research. The fact that the definition and characterization of exosome types are not yet firmly established makes this situation even worse (9). In order to qualitatively and quantitatively evaluate exosomes with cells origins, and thus boost the development of corresponding microfluidic systems, more novel technologies are urgently needed for comprehensively characterizing the surface and intravesicular compositions of exosomes.

cNAs

Gene expression profiles have shown dramatic correlations with tumor development and progression. Genetic changes can thus be utilized as biomarkers for the detection and diagnosis of cancer. Recently developed microfluidic systems for the separation and analysis of nucleic acids are summarized in Table 3, demonstrating the potential to develop point-of-care microfluidic devices capable of being used as liquid biopsies. By integrating and miniaturizing these progresses into microfluidic systems, many advantages including low cost, automation, fast processing time, high throughput, and reduced contamination are realized compared to their conventional macroscale counterparts. Examination of nucleic acids molecules with microfluidic operations has also enabled the emergence of new analysis platforms, especially for clinical translations (180).

Although the development of microfluidic techniques for nucleic acids analysis has advanced significantly, there is still great room for the techniques themselves and the integration capabilities with other processes. For example, nucleic acids are generally separated through extraction process, which can compromise their integrity and result in analysis errors. The ability to achieve complete extraction efficiency from complex samples has also yet to be realized. These issues limit the utility of nucleic acids as biomarkers and are further troublesome for their clinical applications. Therefore, faster and gentler extraction protocols that help to maintain sample integrity and maximize yield efficiency will be crucial to realize the full potential of genetic mapping and single-molecule sequencing technologies. Standardizing sample collection and processing protocols is also important for the development of more reliable and efficient microfluidic devices. In addition, since the separation of nucleic acids is quite difficult and less efficient, an alternative based on separation-free techniques was developed for nucleic acids analysis. Few of these integrated microfluidic devices that are summarized in Table 3 can be able to handle raw samples and guide them through direct detection apparatus. This will be an appealing technique toward developing truly point-of-care microfluidic devices. Furthermore, it is noteworthy that the profiles of genetic mutations in different tumors are much more complicated than we can imagine, and the heterogeneity features make it even more difficult to identify key genetic information of cancer that could provide sufficient diagnostic utility. This calls for more efficient integrated genetic and microfluidic techniques in terms of performance and precision.

CONCLUSIONS

Cancer-derived cells, exosomes and nucleic acids represent typical circulating biomarkers that can be used as noninvasive liquid biopsies for the diagnosis and treatment of cancer-related diseases. Microfluidic technologies endow unique opportunities to achieve the unprecedented spatio-temporal control of these circulating tumor biomarkers. Although the research and development of microfluidic systems for cancer theranostics are relatively recent, a number of studies have already demonstrated their superior performance in separating and identifying these biomarkers from various sources. The next few years will certainly witness even more intense development of microfluidic systems for biomarkers separation, characterization and detection.

However, many challenges still remain and demand persistent attention before clinical translation is feasible. Firstly, the circulating tumor biomarkers are relatively rare and extremely heterogeneous, making their analysis inherently difficult. Overcoming this challenge requires the development of combinatorial techniques that can take advantages of multiple unique physical and biochemical properties of tumor biomarkers. Secondly, through highly precise fluid control and automation, significant advances have been made in the burgeoning field of microfluidic biomarker separation and analysis, but many of such systems remain in the proof-of-concept stage.

To fully explore the clinical potential of microfluidics in liquid biopsy, tremendous efforts are still needed to improve the adaptability of the microfluidic technologies to clinical settings and promote the commercialization of the microfluidic systems. Thirdly, the relationship between circulating tumor biomarkers and microfluidics is still not well established. To further advance the development of microfluidics-based clinical biomarkers assays, validation studies to establish the specificity, sensitivity and reproducibility of such tests should be systematically conducted in large cohorts of cancer patients and for multiple cancers of interest. Finally, but not lastly, our understanding of tumor biology is still in its infancy. As discoveries continue to be made on the roles of various circulating biomarkers in tumor burden and progression, more robust and efficient microfluidic systems will be developed to benefit cancer

patients. We anticipate that in the near future, microfluidic technologies will play an increasingly prominent role in the liquid biopsy of cancer, personalized disease diagnosis and beyond.

FUNDING

The authors are grateful for the financial support from the National Institute of Health (NIH) Director's Transformative Research Award (R01HL137157), NSF ECCS-1509369, and Norris Cotton Cancer Center Developmental Funds (Pilot Projects).

REFERENCES

1. Wan, L., Pantel, K., and Kang, Y. (2013) Tumor metastasis: moving new biological insights into the clinic. *Nat. Med*., 19: 1450–1464.
2. Chi, K.R. (2016) The tumour trail left in blood. *Nature*, 532: 269–271.
3. Hyun, K.A., Kim, J., Gwak, H., and Jung, H.I. (2016) Isolation and enrichment of circulating biomarkers for cancer screening, detection, and diagnostics. *Analyst*. 141: 382–92.
4. Kailasa, S.K. and Kang, S.H. (2009) Microchip-based capillary electrophoresis for dna analysis in modern biotechnology: a review. *Sep. Purif. Rev.*, 38: 242–288.
5. Warburg, O. (1956) On the origin of cancer cells. *Science*,123: 309–314.
6. Hynes, R.O. (2011) Metastatic cells will take any help they can get. *Cancer Cell*, 20: 689–690.
7. Myung, J.H. and Hong, S. (2015) Microfluidic devices to enrich and isolate circulating tumor cells. *Lab Chip*, 15:4500–4511.
8. Im, H., Shao, H., Park, Y.I., Peterson, V.M., Castro, C.M., Weissleder, R., and Lee, H. (2014) Label-free detection and molecular profiling of exosomes with a nano-plasmonic sensor. *Nat. Biotechnol*., 32: 490–495.
9. Kowal, J., Tkach, M., and Théry, C. (2014) Biogenesis and secretion of exosomes. *Curr. Opin. Cell Biol*., 29: 116–125.
10. Ren, J., He, W., Zheng, L., and Duan, H. (2016) From structures to functions: insights into exosomes as promising drug delivery vehicles. *Biomater. Sci*., 4: 910–921.
11. Mandel, P. and Metais, P. (1948) Les acides nucléiques du plasma sanguin chez l'homme. *C. R. Seances Soc. Biol. Ses Fil*., 142: 241–243.
12. Stroun, M., Anker, P., Maurice, P., Lyautey, J., Lederrey, C., and Beljanski, M. (1989) Neoplastic characteristics of the dna found in the plasma of cancer patients. *Oncology*, 46: 318–322.
13. Han, K-H., Han, A., and Frazier, A.B. (2006) Microsystems for isolation and electrophysiological analysis of breast cancer cells from blood. *Biosens. Bioelectron*., 21: 1907–1914.
14. Bettegowda, C., Sausen, M., Leary, R.J., Kinde, I., Wang, Y., Agrawal, N., Bartlett, B.R., Wang, H., Luber, B., Alani, R.M., Antonarakis, E.S., Azad, N.S., Bardelli, A., Brem, H., Cameron, J.L., Lee, C.C., Fecher, L.A., Gallia, G.L., Gibbs, P., Le, D., Giuntoli, R.L., Goggins, M., Hogarty, M. D., Holdhoff, M., Hong, S.-M., Jiao, Y., Juhl, H.H., Kim, J.J., Siravegna, G., Laheru, D.A., Lauricella, C., Lim, M., Lipson, E.J., Marie, S.K.N., Netto, G.J., Oliner, K.S., Olivi, A., Olsson, L., Riggins, G.J., Sartore-Bianchi, A., Schmidt, K., Shih, L.-M., Oba-Shinjo, S.M., Siena, S., Theodorescu, D., Tie, J., Harkins, T.T., Veronese, S., Wang, T.-L., Weingart, J.D., Wolfgang, C.L., Wood, L.D., Xing, D., Hruban, R.H., Wu, J., Allen, P.J., Schmidt, C.M., Choti, M.A., Velculescu, V.E., Kinzler, K.W., Vogelstein, B., Papadopoulos, N., and Diaz, L.A. (2014) Detection of circulating tumor dna in early- and late-stage human malignancies. *Sci. Transl. Med*., 6: 224ra24.
15. Siravegna, G. and Bardelli, A. (2016) Blood circulating tumor dna for non-invasive genotyping of colon cancer patients. *Mol. Oncol*., 10: 475–480.
16. Bellassai, N. and Spoto, G. (2016) Biosensors for liquid biopsy: circulating nucleic acids to diagnose and treat cancer. *Anal. Bioanal. Chem*., 408: 7255–7264.
17. Nahavandi, S., Baratchi, S., Soffe, R., Tang, S-Y., Nahavandi, S., Mitchell, A., and Khoshmanesh, K. (2014) Microfluidic platforms for biomarker analysis. *Lab Chip*, 14: 1496–1514.
18. Lee, R.C., Feinbaum, R.L., and Ambros, V. (1993) The c. elegans heterochronic gene lin-4 encodes small rnas with antisense complementarity to lin-14. *Cell*, 75: 843–854.
19. Allegra, A., Alonci, A., Campo, S., Penna, G., Petrungaro, A., Gerace, D., and Musolino, C. (2012) Circulating micrornas: new biomarkers in diagnosis, prognosis and treatment of cancer (review). *Int. J. Oncol*., 41: 1897–1912.
20. Liu, K.J., Brock, M.V., Shih, I., and Wang, T. (2010) Decoding circulating nucleic acids in human serum using microfluidic single molecule spectroscopy. *J. Am. Chem. Soc*., 132: 5793–5798.
21. Friedrich, S.M., Zec, H.C., and Wang, T-H. (2016) Analysis of single nucleic acid molecules in micro- and nano-fluidics. *Lab Chip*, 16: 790–811.
22. Haeberle, S. and Zengerle, R. (2007) Microfluidic platforms for lab-on-a-chip applications. *Lab Chip*, 7: 1094–1110.
23. Livak-Dahl, E., Sinn, I., and Burns, M. (2011) Microfluidic chemical analysis systems. *Annu. Rev. Chem. Biomol. Eng*., 2: 325–353.
24. Lisowski, P. and Zarzycki, P.K. (2013) Microfluidic paper-based analytical devices (μpads) and micro total analysis systems (μtas): development, applications and future trends. *Chromatographia*, 76: 1201–1214.
25. Faustino, V., Catarino, S.O., Lima, R., and Minas, G. (2015) Biomedical microfluidic devices by using low-cost fabrication techniques: a review. *J. Biomech*., 49: 2280–2292.
26. Alix-Panabières, C. and Pantel, K. (2014) Challenges in circulating tumour cell research. *Nat. Rev. Cancer*, 14: 623–631.
27. Cima, I., Wen Yee, C., Iliescu, F.S., Min Phyo, W., Hon Lim, K., Iliescu, C., and Han Tan, M. (2013) Label-free isolation of circulating tumor cells in microfluidic devices: current research and perspectives. *Biomicrofluidics*, 7: 011810.
28. Hosokawa, M., Hayata, T., Fukuda, Y., Arakaki, A., Yoshino, T., Tanaka, T., and Matsunaga, T. (2010) Size-selective microcavity array for rapid and efficient detection of circulating tumor cells. *Anal. Chem*., 82: 6629–6635.
29. Zheng, S., Lin, H., Liu, J-Q., Balic, M., Datar, R., Cote, R. J., and Tai, Y.-C. (2007) Membrane microfilter device for selective capture, electrolysis and genomic analysis of human circulating tumor cells. *J. Chromatogr. A*, 1162: 154–161.
30. Hosokawa, M., Yoshikawa, T., Negishi, R., Yoshino, T., Koh, Y., Kenmotsu, H., Naito, T., Takahashi, T., Yamamoto, N., Kikuhara, Y., Kanbara, H., Tanaka, T., Yamaguchi, K., and Matsunaga, T. (2013) Microcavity array system for size-based enrichment of circulating tumor cells from the blood of patients with small-cell lung cancer. *Anal. Chem*., 85: 5692–5698.
31. Loutherback, K., D'Silva, J., Liu, L., Wu, A., Austin, R.H., and Sturm, J.C. (2012) Deterministic separation of cancer cells from blood at 10 ml/min. *AIP Adv*., 2: 42107.
32. Liu, Z., Huang, F., Du, J., Shu, W., Feng, H., Xu, X., and Chen, Y. (2013) Rapid isolation of cancer cells using microfluidic deterministic lateral displacement structure. *Biomicrofluidics*, 7: 011801.
33. Mohamed, H., Murray, M., Turner, J.N., and Caggana, M. (2009) Isolation of tumor cells using size and deformation. *J. Chromatogr. A*, 1216: 8289–8295.

34. Tan, S.J., Yobas, L., Lee, G.Y.H., Ong, C.N., and Lim, C.T. (2009) Microdevice for the isolation and enumeration of cancer cells from blood. *Biomed. Microdevices*, 11: 883–892.
35. Tan, S.J., Lakshmi, R.L., Chen, P., Lim, W-T., Yobas, L., and Lim, C. T. (2010) Versatile label free biochip for the detection of circulating tumor cells from peripheral blood in cancer patients. *Biosens. Bioelectron*., 26: 1701–1705.
36. Lv, P., Tang, Z., Liang, X., Guo, M., and Han, R.P.S. (2013) Spatially gradated segregation and recovery of circulating tumor cells from peripheral blood of cancer patients. *Biomicrofluidics*, 7: 034109.
37. Di Carlo, D. (2009) Inertial microfluidics. *Lab Chip*, 9: 3038–3046.
38. Gossett, D.R., Weaver, W.M., Mach, A.J., Hur, S.C., Tse, H.T.K., Lee, W., Amini, H., and Di Carlo, D. (2010) Label-free cell separation and sorting in microfluidic systems. *Anal. Bioanal. Chem*., 397: 3249–3267.
39. Bhagat, A.A.S., Hou, H.W., Li, L.D., Lim, C.T., and Han, J. (2011) Pinched flow coupled shear-modulated inertial microfluidics for high-throughput rare blood cell separation. *Lab Chip*, 11: 1870–1878.
40. Hur, S.C., Mach, A.J., and Di Carlo, D. (2011) High-throughput size-based rare cell enrichment using microscale vortices. *Biomicrofluidics*, 5: 022206.
41. Mach, A.J., Kim, J.H., Arshi, A., Hur, S.C., and Di Carlo, D. (2011) Automated cellular sample preparation using a centrifuge-on-a-chip. *Lab Chip*, 11: 2827–2834.
42. Moon, H-S., Kwon, K., Hyun, K-A., Sim, T.S., Park, J.C., Lee, J.G., and Jung, H.I. (2013) Continual collection and re-separation of circulating tumor cells from blood using multi-stage multi-orifice flow fractionation. *Biomicrofluidics*, 7: 014105.
43. Sun, J., Li, M., Liu, C., Zhang, Y., Liu, D., Liu, W., Hu, G., and Jiang, X. (2012) Double spiral microchannel for label-free tumor cell separation and enrichment. *Lab Chip*, 12: 3952.
44. Sun, J., Liu, C., Li, M., Wang, J., Xianyu, Y, Hu, G., and Jiang, X. (2013) Size-based hydrodynamic rare tumor cell separation in curved microfluidic channels. *Biomicrofluidics*, 7: 011802.
45. Warkiani, M.E., Guan, G., Luan, K.B., Lee, W.C., Bhagat, A.A.S., Kant Chaudhuri, P., Tan, D.S.-W., Lim, W.T., Lee, S.C., Chen, P.C.Y., Lim, C.T., and Han, J. (2014) Slanted spiral microfluidics for the ultra-fast, label-free isolation of circulating tumor cells. *Lab Chip*, 14: 128–137.
46. Hou, H.W., Warkiani, M.E., Khoo, B.L., Li, Z.R., Soo, R.A., Tan, D. S.-W., Lim, W.-T., Han, J., Bhagat, A.A.S., and Lim, C.T. (2013) Isolation and retrieval of circulating tumor cells using centrifugal forces. *Sci. Rep*., 3: 1259.
47. Zborowski, M. and Chamers, J.J. (2011) Rare cell separation and analysis by magnetic sorting. *Anal. Chem*., 83: 8050–8056.
48. Augustsson, P., Magnusson, C., Nordin, M., Lilja, H., and Laurell, T. (2012) Microfluidic, label-free enrichment of prostate cancer cells in blood based on acoustophoresis. *Anal. Chem*., 84: 7954–7962.
49. Ding, X., Peng, Z., Lin, S.C.S., Geri, M., Li, S., Li, P., Chen, Y., Dao, M., Suresh, S., and Huang, T.J. (2014) Cell separation using tilted-angle standing surface acoustic waves. *Proc. Natl. Acad. Sci. U.S.A*., 111: 12992–12997.
50. Li, P., Mao, Z., Peng, Z., Zhou, L., Chen, Y., Huang, P.-H., Truica, C. I., Drabick, J.J., El-Deiry, W.S., Dao, M., Suresh, S., and Huang, T.J. (2015) Acoustic separation of circulating tumor cells. *Proc. Natl. Acad. Sci. U.S.A*., 112: 4970–4975.
51. Kim, M.S., Sim, T.S., Kim, Y.J., Kim, S.S., Jeong, H., Park, J.-M., Moon, H.-S., Kim, S.I., Gurel, O., Lee, S.S., Lee, J.-G., and Park, J.C. (2012) Ssa-moa: a novel ctc isolation platform using selective size amplification (ssa) and a multi-obstacle architecture (moa) filter. *Lab Chip*, 12: 2874–2880.
52. Pethig, R. (2010) Dielectrophoresis: status of the theory, technology, and applications. *Biomicrofluidics*, 4: 022811.
53. Huang, Y., Yang, J., Wang, X-B., Becker, F.F., and Gascoyne, P.R.C. (1999) The removal of human breast cancer cells from hematopoietic cd34 + stem cells by dielectrophoretic field-flow-fractionation. *J. Hematother. Stem Cell Res*., 8: 481–490.
54. Yang, J., Huang, Y., Wang, X.B., Becker, F.F., and Gascoyne, P.R. (1999) Cell separation on microfabricated electrodes using dielectrophoretic/gravitational field-flow fractionation. *Anal. Chem*., 71: 911–918.
55. Wang, X-B., Yang, J., Huang, Y., Vykoukal, J., Becker, F.F., and Gascoyne, P.R.C. (2000) Cell separation by dielectrophoretic field-flow-fractionation. *Anal. Chem*., 72: 832–839.
56. Gascoyne, P.R.C., Noshari, J., Anderson, T.J., and Becker, F.F. (2009) Isolation of rare cells from cell mixtures by dielectrophoresis. *Electrophoresis*, 30: 1388–1398.
57. Sabuncu, A.C., Liu, J.A., Beebe, S.J., and Beskok, A. (2010) Dielectrophoretic separation of mouse melanoma clones. *Biomicrofluidics*, 4: 021101.
58. Cheng, J., Sheldon, E.L., Wu, L., Heller, M.J., and O'Connell, J.P. (1998) Isolation of cultured cervical carcinoma cells mixed with peripheral blood cells on a bioelectronic chip. *Anal. Chem*., 70: 2321–2326.
59. Huang, Y., Joo, S., Duhon, M., Heller, M., Wallace, B., and Xu, X. (2002) Dielectrophoretic cell separation and gene expression profiling on microelectronic chip arrays. *Anal. Chem*., 74: 3362–3371.
60. Altomare, L., Borgatti, M., Medoro, G., Manaresi, N., Tartagni, M., Guerrieri, R., and Gambari, R. (2003) Levitation and movement of human tumor cells using a printed circuit board device based on software-controlled dielectrophoresis. *Biotechnol. Bioeng*., 82: 474–479.
61. Park, J., Kim, B., Choi, S.K., Hong, S., Lee, S.H., and Lee, K-I. (2005) An efficient cell separation system using 3d-asymmetric microelectrodes. *Lab Chip*, 5: 1264–1270.
62. An, J., Lee, J., Lee, S.H., Park, J., and Kim, B. (2009) Separation of malignant human breast cancer epithelial cells from healthy epithelial cells using an advanced dielectrophoresis-activated cell sorter (dacs). *Anal. Bioanal. Chem*., 394: 801–809.
63. Yang, F., Yang, X., Jiang, H., Bulkhaults, P., Wood, P., Hrushesky, W., and Wang, G. (2010) Dielectrophoretic separation of colorectal cancer cells. *Biomicrofluidics*, 4: 013204.
64. Huang, Y., Wang, X.B., Becker, F.F., and Gascoyne, P.R. (1997) Introducing dielectrophoresis as a new force field for field-flow fractionation. *Biophys. J*., 73: 1118–1129.
65. Moon, H-S., Kwon, K., Kim, S-I., Han, H., Sohn. J., Lee, S., and Jung, H.-I. (2011) Continuous separation of breast cancer cells from blood samples using multi-orifice flow fractionation (moff) and dielectrophoresis (dep). *Lab Chip*, 11: 1118–1125.
66. Shafiee, H., Caldwell, J.L., Sano, M.B., and Davalos, R.V. (2009) Contactless dielectrophoresis: a new technique for cell manipulation. *Biomed. Microdevices*, 11: 997–1006.
67. Henslee, E.A., Sano, M.B., Rojas, A.D., Schmelz, E.M., and Davalos, R.V. (2011) Selective concentration of human cancer cells using contactless dielectrophoresis. *Electrophoresis*, 32: 2523–2529.
68. Gupta, V., Jafferji, I., Garza, M., Melnikova, V.O., Hasegawa, D.K., Pethig, R., and Davis, D.W. (2012) Apostream^{TM}, a new dielectrophoretic device for antibody independent isolation and recovery of viable cancer cells from blood. *Biomicrofluidics*, 6: 024133.
69. Hughes, A.D., Mattison, J., Western, L.T., Powderly, J.D., Greene, B. T., and King, M.R. (2012) Microtube device for selectin-mediated capture of viable circulating tumor cells from blood. *Clin. Chem*., 58: 846–853.
70. Wang, S., Liu, K., Liu, J., Yu, Z.T.F., Xu, X., Zhao, L., Lee, T., Lee, E.K., Reiss, J., Lee, Y.K., Chung, L.W.K., Huang, J., Rettig, M., Seligson, D., Duraiswamy, K.N., Shen, C.K.F., and Tseng, H.R.

(2011) Highly efficient capture of circulating tumor cells by using nanostructured silicon substrates with integrated chaotic micromixers. *Angew. Chem. Int. Ed*., 50: 3084–3088.
71. Dharmasiri, U., Njoroge, S.K., Witek, M.A., Adebiyi, M.G., Kamande, J.W., Hupert, M.L., Barany, F., and Soper, S.A. (2011) High-throughput selection, enumeration, electrokinetic manipulation, and molecular profiling of low-abundance circulating tumor cells using a microfluidic system. *Anal. Chem*., 83: 2301–2309.
72. Adams, A.A., Okagbare, P.I., Feng, J., Hupert, M.L., Patterson, D., Gottert, J., McCarley, R. L., Nikitopoulos, D., Murphy, M.C., and Soper, S.A. (2008) Highly efficient circulating tumor cell isolation from whole blood and label-free enumeration using polymer-based microfluidics with an integrated conductivity sensor. *J. Am. Chem. Soc*., 130: 8633–8641.
73. Stott, S.L., Hsu, C-H., Tsukrov, D.I., Yu, M., Miyamoto, D.T., Waltman, B.A., Rothenberg, S.M., Shah, A.M., Smas, M.E., Korir, G.K., Floyd, F.P., Gilman, A.J., Lord, J.B., Winokur, D., Springer, S., Irimia, D., Nagrath, S., Sequist, L.V., Lee, R.J., Isselbacher, K.J., Maheswaran, S., Haber, D.A., and Toner, M. (2010) Isolation of circulating tumor cells using a microvortex-generating herringbone-chip. *Proc. Natl. Acad. Sci. U.S.A*., 107: 18392–18397.
74. Nagrath, S., Sequist, L.V., Maheswaran, S., Bell, D.W., Irimia, D., Ulkus, L., Smith, M.R., Kwak, E.L., Digumarthy, S., Muzikansky, A., Ryan, P., Balis, U.J., Tompkins, R.G., Haber, D.A., and Toner, M. (2007) Isolation of rare circulating tumour cells in cancer patients by microchip technology. *Nature*, 450: 1235–1239.
75. Liu, Z., Zhang, W., Huang, F., Feng, H., Shu, W., Xu, X., and Chen, Y. (2013) High throughput capture of circulating tumor cells using an integrated microfluidic system. *Biosens. Bioelectron*., 47:113–119.
76. Wang, S., Wang, H., Jiao, J., Chen, K.J., Owens, G.E., Kamei, K.I., Sun, J., Sherman, D.J., Behrenbruch, C.P., Wu, H., and Tseng, H.R. (2009) Three-dimensional nanostructured substrates toward efficient capture of circulating tumor cells. *Angew. Chem. Int. Ed*., 48: 8970–8973.
77. Kang, J.H., Krause, S., Tobin, H., Mammoto, A., Kanapathipillai, M., and Ingber, D.E. (2012) A combined micromagnetic-microfluidic device for rapid capture and culture of rare circulating tumor cells. *Lab Chip*, 12: 2175–2181.
78. Sivagnanam, V., Song, B., Vandevyver, C., Bünzli, J.C.G., and Gijs, M.A.M. (2010) Selective breast cancer cell capture, culture, and immunocytochemical analysis using self-assembled magnetic bead patterns in a microfluidic chip. *Langmuir*, 26: 6091–6096.
79. Fais, S., O'Driscoll, L., Borras, F.E., Buzas, E., Camussi, G., Cappello, F., Carvalho, J., Cordeiro da Silva, A., Del Portillo, H., El Andaloussi, S., Ficko Trček, T., Furlan, R., Hendrix, A., Gursel, I., Kralj-Iglic, V., Kaeffer, B., Kosanovic, M., Lekka, M.E., Lipps, G., Logozzi, M., Marcilla, A., Sammar, M., Llorente, A., Nazarenko, I., Oliveira, C., Pocsfalvi, G., Rajendran, L., Raposo, G., Rohde, E., Siljander, P., van Niel, G., Vasconcelos, M.H., Yáñez-Mó, M., Yliperttula, M.L., Zarovni, N., Zavec, A.B., and Giebel, B. (2016) Evidence-based clinical use of nanoscale extracellular vesicles in nanomedicine. *ACS Nano*, 10: 3886–3899.
80. Phillips, J.A., Xu, Y., Xia, Z., Fan, Z.H., and Tan, W. (2009) Enrichment of cancer cells using aptamers immobilized on a microfluidic channel. *Anal. Chem*., 81: 1033–1039.
81. Xu, Y., Phillips, J.A., Yan, J., Li, Q., Fan, Z.H., and Tan, W. (2009) Aptamer-based microfluidic device for enrichment, sorting, and detection of multiple cancer cells. *Anal. Chem*., 81: 7436–7442.
82. Zhu, Y., Kekalo, K., Ndong, C., Huang, Y., Shubitidze, F., Griswold, K.E., Baker, I., and Zhang, J.X.J. (2016) Magnetic-nanoparticle-based immunoassays-on-chip: materials synthesis, surface functionalization, and cancer cell screening. *Adv. Funct. Mater*., 26: 3953–3972.
83. Chen, P., Huang, Y., Hoshino, K., and Zhang, J.X.J. (2014) Multiscale immunomagnetic enrichment of circulating tumor cells: from tubes to microchips. *Lab Chip*, 14: 446–458.
84. Hoshino, K., Huang, Y-Y., Lane, N., Huebschman, M., Uhr, J.W., Frenkel, E.P., and Zhang, J.X.J. (2011) Microchip-based immunomagnetic detection of circulating tumor cells. *Lab Chip*, 11: 3449–3457.
85. Huang, Y.Y., Hoshino, K., Chen, P., Wu, C.H., Lane, N., Huebschman, M., Liu, H., Sokolov, K., Uhr, J.W., Frenkel, E.P., and Zhang, J.X.J. (2013) Immunomagnetic nanoscreening of circulating tumor cells with a motion controlled microfluidic system. *Biomed. Microdevices*, 15: 673–681.
86. Hoshino, K., Chen, P., Huang, Y.Y., and Zhang, J.X.J. (2012) Computational analysis of microfluidic immunomagnetic rare cell separation from a particulate blood flow. *Anal. Chem*., 84: 4292–4299.
87. Huang, Y., Chen, P., Wu, C., Hoshino, K., Sokolov, K., Lane, N., Liu, H., Huebschman, M., Frenkel, E., and Zhang, J.X.J. (2015) Screening and molecular analysis of single circulating tumor cells using micromagnet array. *Sci. Rep*., 5: 16047.
88. Chen, P., Huang, Y.Y., Bhave, G., Hoshino, K., and Zhang, J.X.J. (2016) Inkjet-print micromagnet array on glass slides for immunomagnetic enrichment of circulating tumor cells. *Ann. Biomed. Eng*., 44: 1710–1720.
89. Ng, E., Hoshino, K., and Zhang, J.X.J. (2013) Microfluidic immunodetection of cancer cells via site-specific microcontact printing of antibodies on nanoporous surface. *Methods*, 63: 266–275.
90. Chen, P., Huang, Y-Y., Hoshino, K., and Zhang, J.X.J. (2015) Microscale magnetic field modulation for enhanced capture and distribution of rare circulating tumor cells. *Sci. Rep*., 5: 8745.
91. Wu, C.H., Huang, Y.Y., Chen, P., Hoshino, K., Liu, H., Frenkel, E.P., Zhang, J.X.J., and Sokolov, K.V. (2013) Versatile immunomagnetic nanocarrier platform for capturing cancer cells. *ACS Nano*, 7: 8816–8823.
92. Chen, K.C., Pan, Y.C., Chen, C.L., Lin, C.H., Huang, C.S., and Wo, A.M. (2012) Enumeration and viability of rare cells in a microfluidic disk via positive selection approach. *Anal. Biochem*., 429: 116–123.
93. Ozkumur, E., Shah, A.M., Ciciliano, J.C., Emmink, B.L., Miyamoto, D.T., Brachtel, E., Yu, M., Chen, P., Morgan, B., Trautwein, J., Kimura, A., Sengupta, S., Stott, S.L., Karabacak, N.M., Barber, T. A., Walsh, J.R., Smith, K., Spuhler, P.S., Sullivan, J.P., Lee, R.J., Ting, D.T., Luo, X., Shaw, A.T., Bardia, A., Sequist, L.V, Louis, D.N., Maheswaran, S., Kapur, R., Haber, D.A., and Toner, M. (2013) Inertial focusing for tumor antigen-dependent and -independent sorting of rare circulating tumor cells. *Sci. Transl. Med*., 5: 179ra47.
94. Kim, S., Han, S-I., Park, M-J., Jeon, C-W., Joo, Y-D., Choi, I., and Han, K. (2013) Circulating tumor cell microseparator based on lateral magnetophoresis and immunomagnetic nanobeads. *Anal. Chem*., 85: 2779–2786.
95. Park, J.M., Lee, J.Y., Lee, J.G., Jeong, H., Oh, J.M., Kim, Y.J., Park, D., Kim, M.S., Lee, H.J., Oh, J.H., Lee, S.S., Lee, W.Y., and Huh, N. (2012) Highly efficient assay of circulating tumor cells by selective sedimentation with a density gradient medium and microfiltration from whole blood. *Anal. Chem*., 84: 7400–7407.
96. Lin, M.X, Hyun, K.A., Moon, H.S., Sim, T.S., Lee, J.G., Park, J.C., Lee, S.S., and Jung, H.I. (2013) Continuous labeling of circulating tumor cells with microbeads using a vortex micromixer for highly selective isolation. *Biosens. Bioelectron*., 40: 63–67.
97. Kim, M.S., Kim, J., Lee, W., Cho, S.J., Oh, J.M., Lee, J.Y., Baek, S., Kim, Y.J., Sim, T.S., Lee, H.J., Jung, G.E., Kim, S.I., Park, J.M., Oh, J.H., Gurel, O., Lee, S.S., and Lee, J.G. (2013) A trachea-inspired bifurcated microfilter capturing viable circulating tumor cells via altered biophysical properties as measured by atomic force microscopy. *Small*, 9: 3103–3110.
98. Liu, Z., Fusi, A., Klopocki, E., Schmittel, A., Tinhofer, I., Nonnenmacher, A., and Keilholz, U. (2011) Negative enrichment by immunomagnetic nanobeads for unbiased characterization of circulating tumor cells from peripheral blood of cancer patients. *J. Transl. Med*., 9: 70.

99. Hyun, K.A., Lee, T.Y., and Jung, H.I. (2013) Negative enrichment of circulating tumor cells using a geometrically activated surface interaction chip. *Anal. Chem*., 85: 4439–4445.
100. Diéguez, L., Winter, M.A., Pocock, K.J., Bremmell, K.E., and Thierry, B. (2015) Efficient microfluidic negative enrichment of circulating tumor cells in blood using roughened pdms. *Analyst*, 140: 3565–3572.
101. Chen, C-L., Chen, K-C., Pan, Y-C., Lee, T-P., Hsiung, L-C., Lin, C.-M., Chen, C.-Y., Lin, C.-H., Chiang, B.-L., and Wo, A.M. (2011) Separation and detection of rare cells in a microfluidic disk via negative selection. *Lab Chip*, 11: 474–483.
102. Lu, Y., Liang, H., Yu, T., Xie, J., Chen, S., Dong, H., Sinko, P.J., Lian, S., Xu, J., Wang, J., Yu, S., Shao, J., Yuan, B., Wang, L., and Jia, L. (2015) Isolation and characterization of living circulating tumor cells in patients by immunomagnetic negative enrichment coupled with flow cytometry. *Cancer*, 121: 3036–3045.
103. Sajay, B.N.G., Chang, C.P., Ahmad, H., Khuntontong, P., Wong, C.C., Wang, Z., Puiu, P. D., Soo, R., and Rahman, A.R.A. (2014) Microfluidic platform for negative enrichment of circulating tumor cells. *Biomed. Microdevices*, 16: 537–548.
104. Bhuvanendran Nair Gourikutty, S., Chang, C-P., and Poenar, D.P. (2016) An integrated on-chip platform for negative enrichment of tumour cells. *J. Chromatogr. B*, 1028: 153–164.
105. Karabacak, N.M., Spuhler, P.S., Fachin, F., Lim, E.J., Pai, V., Ozkumur, E., Martel, J.M., Kojic, N., Smith, K., Chen, P., Yang, J., Hwang, H., Morgan, B., Trautwein, J., Barber, T.A., Stott, S.L., Maheswaran, S., Kapur, R., Haber, D.A., and Toner, M. (2014) Microfluidic, marker-free isolation of circulating tumor cells from blood samples. *Nat. Protoc*., 9: 694–710.
106. Kwon, K.W., Choi, S.S., Lee, S.H., Kim, B., Lee, S.N., Park, M.C., Kim, P., Hwang, S.Y., and Suh, K.Y. (2007) Label-free, microfluidic separation and enrichment of human breast cancer cells by adhesion difference. *Lab Chip*, 7: 1461–1468.
107. Kuo, J.S., Zhao, Y., Schiro, P.G., Ng, L., Lim, D.S.W., Shelby, J.P., and Chiu, D.T. (2010) Deformability considerations in filtration of biological cells. *Lab Chip*, 10: 837–842.
108. Zheng, S., Lin, H.K., Lu, B., Williams, A., Datar, R., Cote, R.J., and Tai, Y.C. (2011) 3d microfilter device for viable circulating tumor cell (ctc) enrichment from blood. *Biomed. Microdevices*, 13: 203–213.
109. Bhagat, A.A.S., Hou, H.W., Li, L.D., Lim, C.T., and Han, J.H. (2011) Dean flow fractionation (DFF) isolation of circulating tumor cells (CTCs) from blood. *15th International Conference on Miniaturized Systems for Chemistry and Life Sciences. Seattle, Washington, USA*, 524–526.
110. Hosokawa, M., Kenmotsu, H., Koh, Y., Yoshino, T., Yoshikawa, T., Naito, T., Takahashi, T., Murakami, H., Nakamura, Y., Tsuya, A., Shukuya, T., Ono, A., Akamatsu, H., Watanabe, R., Ono, S., Mori, K., Kanbara, H., Yamaguchi, K., Tanaka, T., Matsunaga, T., and Yamamoto, N. (2013) Size-based isolation of circulating tumor cells in lung cancer patients using a microcavity array system. *PLoS One*, 8: e67466.
111. Becker, F.F., Wang, X.B., Huang, Y., Pethig, R., Vykoukal, J., and Gascoyne, P.R.C. (1994) The removal of human leukaemia cells from blood using interdigitated microelectrodes. *J. Phys. D Appl. Phys*., 27: 2659–2662.
112. Becker, F.F., Wang, X.B., Huang, Y., Pethig, R., Vykoukal, J., and Gascoyne, P.R. (1995) Separation of human breast cancer cells from blood by differential dielectric affinity. *Proc. Natl. Acad. Sci. U.S.A*., 92: 860–864.
113. Gascoyne, P.R.C., Wang, X.B., Huang, Y., and Becker, R.F. (1997) Dielectrophoretic separation of cancer cells from blood. *IEEE T. Ind. Appl*., 33: 670–678.
114. Das, C.M., Becker, F., Vernon, S., Noshari, J., Joyce, C., and Gascoyne, P. R.C. (2005) Dielectrophoretic segregation of different human cell types on microscope slides dielectrophoretic segregation of different human cell types on microscope slides. *Anal. Chem*., 77: 2708–2719.
115. Tai, C.H., Hsiung, S.K., Chen, C.Y., Tsai, M.L., and Lee, G.B. (2007) Automatic microfluidic platform for cell separation and nucleus collection. *Biomed. Microdevices*, 9: 533–543.
116. Kim, U., Shu, C-W., Dane, K.Y., Daugherty, P.S., Wang, J.Y.J., and Soh, H.T. (2007) Selection of mammalian cells based on their cell-cycle phase using dielectrophoresis. *Proc. Natl. Acad. Sci. U.S.A*., 104: 20708–20712.
117. Cristofanilli, M., Krishnamurthy, S., Das, C.M., Reuben, J.M., Spohn, W., Noshari, J., Becker, F., and Gascoyne, P.R. (2008) Dielectric cell separation of fine needle aspirates from tumor xenografts. *J. Sep. Sci*., 31: 3732–3739.
118. Kang, Y., Li, D., Kalams, S.A., and Eid, J.E. (2008) Dc-dielectrophoretic separation of biological cells by size. *Biomed. Microdevices*, 10: 243–249.
119. Kostner, S., van den Driesche, S., Witarski, W., Pastorekova, S., and Vellekoop, M.J. (2010) Guided dielectrophoresis: a robust method for continuous particle and cell separation. *IEEE Sens. J*., 10: 1440–1446.
120. Alazzam, A., Stiharu, I., Bhat, R., and Meguerditchian, A.N. (2011) Interdigitated comb-like electrodes for continuous separation of malignant cells from blood using dielectrophoresis. *Electrophoresis*. 32: 1327–1336.
121. Huang, S-B., Wu M-H., Lin, Y-H., Hsieh, C-H., Yang, C-L., Lin, H.-C., Tseng, C.-P., and Lee, G.-B. (2013) High-purity and label-free isolation of circulating tumor cells (ctcs) in a microfluidic platform by using optically-induced-dielectrophoretic (odep) force. *Lab Chip*, 13: 1371–1383.
122. Takao, M. and Takeda, K. (2011) Enumeration, characterization, and collection of intact circulating tumor cells by cross contamination-free flow cytometry. *Cytom. A*, 79: 107–117.
123. Mittal, S., Wong, I.Y., Deen, W.M., and Toner, M. (2012) Antibody-functionalized fluid-permeable surfaces for rolling cell capture at high flow rates. *Biophys. J*., 102: 721–730.
124. Schiro, P.G., Zhao, M., Kuo, J.S., Koehler, K.M., Sabath, D.E., and Chiu, D.T. (2012) Sensitive and high-throughput isolation of rare cells from peripheral blood with ensemble-decision aliquot ranking. *Angew. Chem. Int. Ed*., 51: 4618–4622.
125. Kralj, J.G., Arya, C., Tona, A., Forbes, T.P., Munson, M.S., Sorbara, L., Srivastava, S., and Forry, S.P. (2012) A simple packed bed device for antibody labelled rare cell capture from whole blood. *Lab Chip*, 12: 4972–4975.
126. Ko, J., Carpenter, E., and Issadore, D. (2015) Detection and isolation of circulating exosomes and microvesicles for cancer monitoring and diagnostics using micro-/nano-based devices. *Analyst*, 141:450–460.
127. He, M. and Zeng, Y. (2016) Microfluidic exosome analysis toward liquid biopsy for cancer. *J. Lab. Autom*., 21: 599–608.
128. Wang, Z., Wu, H., Fine, D., Schmulen, J., Hu, Y., Godin, B., Zhang, J. X.J., and Liu, X. (2013) Ciliated micropillars for the microfluidic-based isolation of nanoscale lipid vesicles. *Lab Chip*, 13: 2879–2882.
129. Davies, R.T., Kim, J., Jang, S.C., Choi, E-J., Gho, Y.S., and Park, J. (2012) Microfluidic filtration system to isolate extracellular vesicles from blood. *Lab Chip*, 12: 5202–5210.
130. Santana, S.M., Antonyak, M.A., Cerione, R.A., and Kirby, B.J. (2014) Microfluidic isolation of cancer-cell-derived microvesicles from hetergeneous extracellular shed vesicle populations. *Biomed. Microdevices*, 16: 869–877.
131. Jo, W., Jeong, D., Kim, J., Cho, S., Jang, S.C., Han, C., Kang, J.Y., Gho, Y.S., and Park, J. (2014) Microfluidic fabrication of cell-derived nanovesicles as endogenous rna carriers. *Lab Chip*, 14: 1261–1269.
132. Lee, K., Shao, H., Weissleder, R., and Lee, H. (2015) Acoustic purification of extracellular microvesicles. *ACS Nano*, 9: 2321–2327.
133. Maiolo, D., Paolini, L., Di Noto, G., Zendrini, A., Berti, D., Bergese, P., and Ricotta, D. (2015) Colorimetric nanoplasmonic assay to determine purity and titrate extracellular vesicles. *Anal. Chem*., 87: 4168–4176.
134. Zhu, L., Wang, K., Cui, J., Liu, H., Bu, X., Ma, H., Wang, W., Gong, H., Lausted, C., Hood, L., Yang, G., and Hu, Z. (2014) Label-free

quantitative detection of tumor-derived exosomes through surface plasmon resonance imaging. *Anal. Chem*., 86: 8857–8864.
135. Chiu, Y., Cai, W., Shih, Y.V., Lian, I., and Lo, Y. (2016) A single-cell assay for time lapse studies of exosome secretion and cell behaviors. *Small*, 12: 3658–3666.
136. Chen, C., Skog, J., Hsu, C., Lessard, R.T., Balaj, L., Wurdinger, T., Carter, B.S., Breakefield, X.O., Toner, M., and Irimia, D. (2010) Microfluidic isolation and transcriptome analysis of serum microvesicles. *Lab Chip*, 10: 505–511.
137. Kanwar, S.S., Dunlay, C.J., Simeone, D.M., and Nagrath, S. (2014) Microfluidic device (exochip) for on-chip isolation, quantification and characterization of circulating exosomes. *Lab Chip*, 14: 1891–1900.
138. Zhang, P., He, M., and Zeng, Y. (2016) Ultrasensitive microfluidic analysis of circulating exosomes using a nanostructured graphene oxide/polydopamine coating. *Lab Chip*, 16: 3033–3042.
139. Vaidyanathan, R., Naghibosadat, M., Rauf, S., Korbie, D., Carrascosa, L.G., Shiddiky, M.J.A., and Trau, M. (2014) Detecting exosomes specifically: a multiplexed device based on alternating current electrohydrodynamic induced nanoshearing. *Anal. Chem*., 86: 11125–11132.
140. Shao, H., Chung, J., Lee, K., Balaj, L., Min, C., Carter, B.S., Hochberg, F.H., Breakefield, X.O., Lee, H., and Weissleder, R. (2015) Chip-based analysis of exosomal mrna mediating drug resistance in glioblastoma. *Nat. Commun*., 6: 6999.
141. Zhao, Z., Yang, Y., Zeng, Y., and He, M. (2016) A microfluidic exosearch chip for multiplexed exosome detection towards blood-based ovarian cancer diagnosis. *Lab Chip*, 16: 489–496.
142. Dudani, J.S., Gossett, D.R., Tse, H.T.K., Lamm, R.J., Kulkarni, R.P., and Carlo, D.D. (2015) Rapid inertial solution exchange for enrichment and flow cytometric detection of microvesicles. *Biomicrofluidics*, 9: 014112.
143. He, M., Crow, J., Roth, M., Zeng, Y., and Godwin, A.K. (2014) Integrated immunoisolation and protein analysis of circulating exosomes using microfluidic technology. *Lab Chip*, 14: 3773–3780.
144. Shao, H., Chung, J., Balaj, L., Charest, A., Bigner, D.D., Carter, B.S., Hochberg, F.H., Breakefield, X.O., Weissleder, R., and Lee, H. (2012) Protein typing of circulating microvesicles allows real-time monitoring of glioblastoma therapy. *Nat. Med*., 18: 1835–1840.
145. Rho, J., Chung, J., Im, H., Liong, M., Shao, H., Castro, C.M., Weissleder, R., and Lee, H. (2013) Magnetic nanosensor for detection and profiling of erythrocyte-derived microvesicles. *ACS Nano*, 7: 11227–11233.
146. Duarte, G.R.M., Coltro, W.K.T., Borba, J.C., Price, C.W., Landers, J. P., and Carrilho, E. (2012) Disposable polyester-toner electrophoresis microchips for dna analysis. *Analyst*, 137: 2692–2698.
147. Reinholt, S.J. and Baeumner, A.J. (2014) Microfluidic isolation of nucleic acids. *Angew. Chem. Int. Ed*., 53: 13988–13981.
148. Ahmad, H., Sutherland, A., Shin, Y.S., Hwang, K., Qin, L., Krom, R.-J., and Heath, J.R. (2011) A robotics platform for automated batch fabrication of high density, microfluidics-based dna microarrays, with applications to single cell, multiplex assays of secreted proteins. *Rev. Sci. Instrum*., 82: 94301.
149. Yu, J., Zhou, J., Sutherland, A., Wei, W., Shin, Y.S., Xue, M., and Heath, J. R. (2014) Microfluidics-based single-cell functional proteomics for fundamental and applied biomedical applications. *Annu. Rev. Anal. Chem*., 7: 275–295.
150. Burns, M.A., Johnson, B.N., Brahmasandra, S.N., Handique, K., Webster, J.R., Krishnan, M., Sammarco, T.S., Man, P.M., Jones, D., Heldsinger, D., Mastrangelo, C.H., and Burke, D.T. 1998. An integrated nanoliter dna analysis device. *Science*, 282: 484–487.
151. Chan, E.Y., Goncalves, N.M., Haeusler, R.A., Hatch, A.J., Larson, J. W., Maletta, A.M., Yantz, G.R., Carstea, E.D., Fuchs, M., Wong, G. G., Gullans, S.R., and Gilmanshin, R. (2004) Dna mapping using microfluidic stretching and single-molecule detection of fluorescent site-specific tags. *Genome Res*., 14: 1137–1146.
152. Dimalanta, E.T., Lim, A., Runnheim, R., Lamers, C., Churas, C., Forrest, D.K., De Pablo, J.J., Graham, M.D., Coppersmith, S.N., Goldstein, S., and Schwartz, D.C. (2004) A microfluidic system for large dna molecule arrays. *Anal. Chem*., 76: 5293–5301.
153. Lehmann, U., Vandevyver, C., Parashar, V.K., and Gijs, M.A.M. (2006) Droplet-based dna purification in a magnetic lab-on-a-chip. *Angew. Chem. Int. Ed*., 45: 3062–3067.
154. Neely, L.A., Patel, S., Garver, J., Gallo, M., Hackett, M., McLaughlin, S., Nadel, M., Harris, J., Gullans, S., and Rooke, J. (2006) A single-molecule method for the quantitation of microrna gene expression. *Nat. Methods*, 3: 41–46.
155. Marcus, J.S., Anderson, W.F., and Quake, S.R. (2006) Microfluidic single-cell mrna isolation and analysis. *Anal. Chem*., 78: 3084–3089.
156. Park, D.S.W., Hupert, M.L., Witek, M.A., You, B.H., Datta, P., Guy, J., Lee, J.B., Soper, S.A., Nikitopoulos, D.E., and Murphy, M.C. (2008) A titer plate-based polymer microfluidic platform for high throughput nucleic acid purification. *Biomed. Microdevices*, 10: 21–33.
157. Mitchell, P.S., Parkin, R.K., Kroh, E.M., Fritz, B.R., Wyman, S.K., Pogosova-Agadjanyan, E.L., Peterson, A., Noteboom, J., O'Briant, K.C., Allen, A., Lin, D.W., Urban, N., Drescher, C.W., Knudsen, B.S., Stirewalt, D.L., Gentleman, R., Vessella, R.L., Nelson, P.S., Martin, D.B., and Tewari, M. (2008) Circulating microrna as stable blood-based markers for cancer detection. *Proc. Natl. Acad. Sci. U.S.A*., 105: 10513–10518.
158. Jo, K., Chen, Y.L., de Pablo, J.J., and Schwartz, D.C. (2009) Elongation and migration of single dna molecules in microchannels using oscillatory shear flows. *Lab Chip*, 9: 2348–2355.
159. Nugen, S.R., Asiello, P.J., and Baeumner, A.J. (2009) Design and fabrication of a microfluidic device for near-single cell mrna isolation using a copper hot embossing master. *Microsyst. Technol*., 15: 477–483.
160. Puleo, C.M. and Wang, T-H. (2009) Microfluidic means of achieving attomolar detection limits with molecular beacon probes. *Lab Chip*, 9: 1065–1072.
161. De, A.F., Gentile, F., Mecarini, F., Das, G., Moretti, M., Candeloro, P., Coluccio, M.L., Cojoc, G., Accardo, A., Liberale, C., Zaccaria, R.P., Perozziello, G., Tirinato, L., Toma, A., Cuda, G., Cingolani, R., and Di Fabrizio, E. (2011) Breaking the diffusion limit with super-hydrophobic delivery of molecules to plasmonic nanofocusing sers structures. *Nat. Photon*., 5: 682–687.
162. Pekin, D., Skhiri, Y., Baret, J-C., Corre, D.L., Mazutis, L., Salem, C. Ben, Millot, F., Harrak, A. El, Hutchison, J. B., Larson, J. W., Link, D. R., Laurent-Puig, P., Griffiths, A. D., and Taly, V. (2011) Quantitative and sensitive detection of rare mutations using droplet-based microfluidics. *Lab Chip*, 11: 2156–2166.
163. Kim, S., Streets, A.M., Lin, R.R., Quake, S.R., Weiss, S., and Majumdar, D.S. (2011) High-throughput single-molecule optofluidic analysis. *Nat. Methods*, 8: 242–245.
164. Zhang, Y., Park, S., Liu, K., Tsuan, J., Yang, S., and Wang, T-H. (2011) A surface topography assisted droplet manipulation platform for biomarker detection and pathogen identification. *Lab Chip*, 11: 398–406.
165. Lam, E.T., Hastie, A., Lin, C., Ehrlich, D., Das, S.K., Austin, M.D., Deshpande, P., Cao, H., Nagarajan, N., Xiao, M., and Kwok, P.Y. (2012) Genome mapping on nanochannel arrays for structural variation analysis and sequence assembly. *Nat. Biotechnol*., 30: 771–776.
166. Xu, W. and Muller, S.J. (2012) Polymer-monovalent salt-induced dna compaction studied via single-molecule microfluidic trapping. *Lab Chip*. 12: 647–651.
167. Schrauder, M.G., Strick, R., Schulz-Wendtland, R., Strissel, P.L., Kahmann, L., Loehberg, C.R., Lux, M.P., Jud, S. M., Hartmann, A., Hein, A., Bayer, C.M., Bani, M.R., Richter, S., Adamietz, B.R., Wenkel, E., Rauh, C., Beckmann, M.W., and Fasching, P.A. (2012) Circulating micro-rnas as potential blood-based markers for early stage breast cancer detection. *PLoS One*, 7: e29770.
168. Goda, T., Masuno, K., Nishida, J., Kosaka, N., Ochiya, T., Matsumoto, A., and Miyahara, Y. (2012) A label-free electrical detection of exosomal micrornas using microelectrode array. *Chem. Commun*., 48: 11942–11944.

169. Zhang, H., Jenkins, G., Zou, Y., Zhu, Z., and Yang, C.J. (2012) Massively parallel single-molecule and single-cell emulsion reverse transcription polymerase chain reaction using agarose droplet microfluidics. *Anal. Chem*., 84: 3599–3606.
170. Rane, T.D., Zec, H.C., Puleo, C., Lee, A.P., and Wang, T-H. (2012) Droplet microfluidics for amplification-free genetic detection of single cells. *Lab Chip*, 12: 3341–3347.
171. Sonnenberg, A., Marciniak, J.Y., Mccanna, J., Krishnan, R., Rassenti, L., Kipps, T.J., and Heller, M.J. (2013) Dielectrophoretic isolation and detection of cfc-dna nanoparticulate biomarkers and virus from blood. *Electrophoresis*, 34: 1076–1084.
172. Reinholt, S.J., Behrent, A., Greene, C., Kalfe, A., and Baeumner, A.J. (2014) Isolation and amplification of mrna within a simple microfluidic lab on a chip. *Anal. Chem*., 86: 849–856.
173. Wei, F., Lin, C-C, Joon, A., Feng, Z., Troche, G., Lira, M.E., Chia, D., Mao, M., Ho, C.-L., Su, W.-C., and Wong, D.T.W. (2014) Noninvasive saliva-based egfr gene mutation detection in patients with lung cancer. *Am. J .Respir. Crit. Care Med*., 190: 1117–1126.
174. Mccanna, J.P., Sonnenberg, A., and Heller, M.J. (2014) Low level epifluorescent detection of nanoparticles and dna on dielectrophoretic microarrays. *J. Biophotonics*., 7: 863–873.
175. Taller, D., Richards, K., Slouka, Z., Senapati, S., Hill, R., Go, D. B., and Chang, H.-C. (2015) On-chip surface acoustic wave lysis and ion-exchange nanomembrane detection of exosomal rna for pancreatic cancer study and diagnosis. *Lab Chip*., 15: 1656–1666.
176. Dias, T.M., Cardoso, F.A., Martins, S.A.M., Martins, V.C., Cardoso, S., Gaspar, J.F., Monteiro, G., and Freitas, P.P. (2016) Implementing a strategy for on-chip detection of cell-free dna fragments using gmr sensors: a translational application in cancer diagnostics using alu elements. *Anal. Methods*., 8: 119–128.
177. Hao, N.J., Li, L., and Tang, F. (2016) Shape matters when engineering mesoporous silica-based nanomedicines. *Biomater. Sci*., 4: 575–591.
178. Hao, N.J., Li, L., and Tang, F. (2017) Roles of particle size, shape and surface chemistry of mesoporous silica nanomaterials on biological systems. *Int. Mater. Rev.*, 62: 57–77.
179. Oosthuyzen, W., Sime, N.E.L., Ivy, J.R., Turtle, E.J., Street, J.M., Pound, J., Bath, L.E., Webb, D.J., Gregory, C.D., Bailey, M.A., and Dear, J.W. (2013) Quantification of human urinary exosomes by nanoparticle tracking analysis. *J. Physiol*., 591: 5833–5842.
180. Fakhoury, J.R., Sisson, J.C., and Zhang, J.X.J. (2009) Microsystems for controlled genetic perturbation of live drosophila embryos: rna interference, development robustness and drug screening. *Microfluid. Nanofluid*., 6: 299–313.